α-Pyrone Derivatives, Tetra/Hexahydroxanthones, and Cyclodepsipeptides from Two Freshwater Fungi

By: Tamam El-Elimat, Huzefa A Raja, Cynthia S. Day, Hana McFeeters, Robert L. McFeeters, and Nicholas H. Oberlies

Tamam El-Elimat, Huzefa A Raja, Cynthia S. Day, Hana McFeeters, Robert L. McFeeters, and Nicholas H. Oberlies. (2017) α-Pyrone Derivatives, Tetra/Hexahydroxanthones, and Cyclodepsipeptides from Two Freshwater Fungi. *Bioorganic & Medicinal Chemistry, 25*(2): 795-804. PMID: 27964996; doi: 10.1016/j.bmc.2016.11.059

Made available courtesy of Elsevier: https://doi.org/10.1016/j.bmc.2016.11.059

Abstract:

Eighteen (**1**–**18**) and seven (**1**, **4**, **6**–**8**, **17** and **18**) compounds were isolated from organic extracts of axenic cultures of two freshwater fungi *Clohesyomyces* sp. and *Clohesyomyces aquaticus* (Dothideomycetes, Ascomycota), respectively. Compounds **1**–**12** belong to the α-pyrone class of natural products, compounds **13** and **14** were tetrahydroxanthones, compounds **15** and **16** were hexahydroxanthones, while compounds **17** and **18** were cyclodepsipeptides. The structures were elucidated using a set of spectroscopic and spectrometric techniques. The absolute configurations of compounds **2**, **3**, **6**, and **7** were assigned via a modified Mosher's ester method using ^{1}H NMR data. The relative configurations of compounds **14**–**16** were determined through NOE data. Compounds **1**, **2**, **6**, **8**, **13**, **14**, and **15** were found to inhibit the essential enzyme bacterial peptidyl-tRNA hydrolase (Pth1), with (**13**; secalonic acid A) being the most potent. Compounds **1** and **4**–**18** were also evaluated for antimicrobial activity against an array of bacteria and fungi but were found to be inactive.

Keywords: Freshwater fungi | α-Pyrones | Tetrahydroxanthones | Cyclodepsipeptides | Bacterial peptidyl-tRNA hydrolase

Article:

1. Introduction

In pursuit of structurally unique and bioactive secondary metabolites from distinct ecological habitats, our group has been interested in fungi, particularly freshwater fungi[1, 2, 3, 4, 5] that inhabit submerged woody and herbaceous substrates in streams and lakes.[6] Freshwater fungi represent a potentially rich, although poorly studied, source of new mycological and chemical diversity.[7, 8]

While working in the Lake Brandt watershed of Greensboro, NC, two related freshwater fungal species, belonging to the genus *Clohesyomyces*, were isolated from submerged wood and accessioned as G100 and G102. Fungal strain G102 biosynthesized 18 compounds belonging to three distinct classes of natural products. Twelve were members of the *α*-pyrone class of secondary metabolites (**1**–**12**), of which five were known [phomopsinone A (**1**), phomopsinone B (**2**), phomopsinone C (**3**), pyrenocine M (**4**), and pyrenocine K (**5**)] and seven were new [6-hydroxy-7-*epi*-phomopsinone A (**6**), 5-deoxy-7-hyrdoxypyrenocine M (**7**), pyrenocine P (**8**), 7-hyrdoxypyrenocine M (**9**), pyrenocine Q (**10**), pyrenocine R (**11**), 5-hydroxyphomopsinone A (**12**)]. Alternatively, four metabolites were tetra/hexahydroxanthones (**13**–**16**), of which one was the known homodimeric tetrahydroxanthone, secalonic acid A (**13**), another was a new natural monomeric tetrahydroxanthone [8-hydroxyblennolide H (**14**)], and two were new monomeric hexahydroxanthones [*cis*-dihydro-8-hydroxyblennolide H (**15**) and *trans*-dihydro-8-hydroxyblennolide H (**16**)]. Finally, also isolated were the two known cyclodepsipeptides [Sch 378161 (**17**) and Sch 217048 (**18**)]. From the perspective of chemical mycology, it was interesting that of these 18 metabolites, the related strain G100 biosynthesized seven overlapping compounds, being **1**, **4**, **6**–**8**, **17** and **18**, which belong to the α-pyrone and cyclodepsipeptide classes of compounds, while the tetra/hexahydroxanthones were biosynthesized only by the G102 strain. Since these related fungi were isolated from the same freshwater habitat, and because they biosynthesized an overlapping series of compounds, the chemical, biological, and mycological data were combined into a single communication.

α-Pyrones have been reported to have varying potency in assays for antifungal, antibacterial, and antialgal activity.[9, 10] Tetrahydroxanthones are an important class of mycotoxins with diverse biological activities, including antitumor, antibacterial, and anti-HIV.[11, 12, 13, 14, 15, 16, 17] The isolated cyclodepsipeptides in this study were reported as selective and competitive human tachykinin receptor (NK_2) antagonists.[18] Given this diversity of biological activities, compounds **1**–**18** were evaluated against a panel of bacteria and fungi. While *in vivo* activity was without prospect, *in vitro* inhibitory activity against the essential enzyme bacterial peptidyl-tRNA hydrolase (Pth1) was observed. Bacterial Pth1 represents a promising new target for antibiotic development[19] for which little is known about small molecule inhibition.[20] Based on this initial screening set, secondary metabolites from fungal cultures could serve as a source of Pth1 inhibitors, providing avenues to better understand inhibitor binding and inhibitor bound states.

2. Results and discussion

The freshwater fungal strains, coded G100 and G102, were ITS sequenced[21] and identified as *Clohesyomyces aquaticus* (Dothideomycetes, Ascomycota) and *Clohesyomyces* sp., respectively. Large-scale solid-phase cultures of G100 and G102 were extracted and partitioned with organic solvents, as described previously.[3, 5] The organic extracts were then purified separately using normal-phase flash chromatography to generate five fractions each, which were then subjected to further purifications using preparative and semipreparative HPLC to yield seven (**1**, **4**, **6**–**8**, **17** and **18**) and 18 compounds (**1**–**18**) from G100 and G102, respectively; all compounds were verified to have >95% purity as measured by UPLC using an evaporative light scattering detector (ELSD) (Fig. S1, Supporting Information). The biosynthetic potential of these

two fungal cultures was broad, as compounds **1**–**12** belonged to the α-pyrone class of natural products, compounds **13**–**16**were tetra/hexahydroxanthones, while compounds **17** and **18** were cyclodepsipeptides.

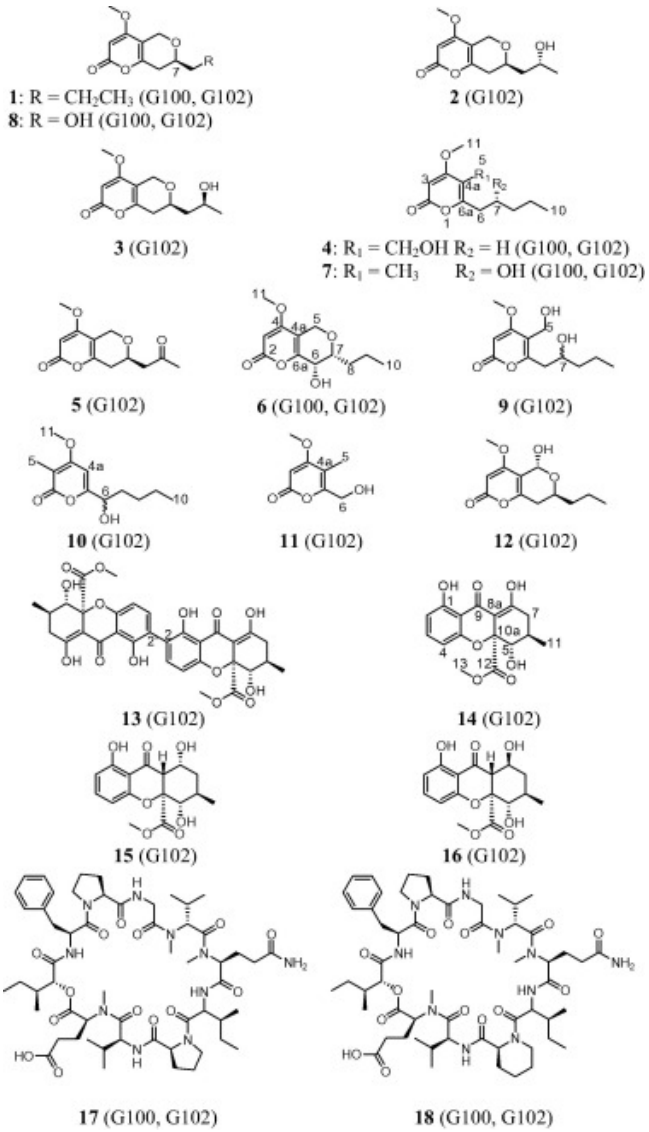

Fig. 1. Structures of metabolites isolated from fungal cultures G100 and G102 (**1**–**18**).

2.1. α-Pyrone derivatives

The NMR and HRESIMS, along with CD and optical rotation data, where appropriate, identified compounds **1** [6.1 mg (G100); 27.8 mg (G102)]; **2** [0.8 mg (G102)], **3** [0.7 mg (G102)], **4** [0.8 mg (G100); 1.7 mg (G102)], and **5** [0.5 mg (G102)] as the known metabolites phomopsinone A,[10] phomopsinone B,[10] phomopsinone C,[10] pyrenocine M,[9] and pyrenocine K,[9] respectively (Figs. 1 and S2–S6, Table S1). Compounds **1** and **4** were first isolated from two different strains of an endophytic *Phomopsis* sp., which were isolated from two different plant hosts.[9, 10] The specific rotation data of **1** was not reported previously and hence provided herein. Epimeric **2** and **3** were first isolated from an endophytic *Phomopsis* sp., which was isolated

from *Santolina chamaecyparissus*.[10] The absolute configuration of **2** was determined by CD spectroscopy and TDDFT calculations.[10] However, due to paucity and insufficient purity of **3**, the researchers were unable to collect CD data to assign the absolute configuration. Hence, they relied on biogenetic considerations and the fact that **2** and **3** were epimers at C-10 to propose the absolute configuration for **3**. No specific rotation data were reported for compounds **2** and **3**. Herein, the absolute configurations of **2** and **3** were confirmed via a modified Mosher's ester method (Fig. 2),[22] the specific rotation data for **2** and **3** and the CD data for **3** were provided as well (Fig. 3). Finally, compound **5** was identified as the known pyrenocine K, which was first isolated from a *Phomopsis* sp., an endophyte of *Cistus salviifolius*.[9] There were some minor differences between the reported and the collected NMR data for **5** (Table S2); however the 2D-NMR and specific rotation data confirmed the structure of **5** as the known pyrenocine K.[9] The NMR data are provided to update the literature (Table 1). CD data have not been reported for compound **5** and hence they are provided (Fig. 3) to confirm the absolute configuration as 7*R*. In short, the characterization data for five of the previously reported α-pyrones have been refined.

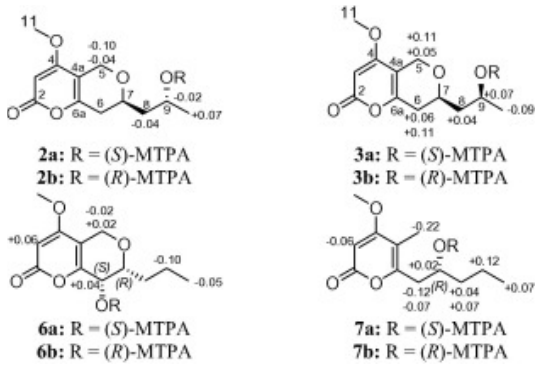

Fig. 2. $\Delta\delta_H$ values [$\Delta\delta$ (in ppm) = $\delta_S - \delta_R$] obtained for (*S*)- and (*R*)-MTPA esters A) **2a** and **2b**, respectively of phomopsinone B (**2**), B) **3a** and **3b**, respectively of phomopsinone C (**3**), C) **6a** and **6b**, respectively of 6-hydroxy-7-*epi*-phomopsinone A (**6**), and D) **7a** and **7b**, respectively of 5-deoxy-7-hyrdoxypyrenocine M (**7**) in pyridine-d_5.

Compound **6** [2.0 mg (G100); 1.2 mg (G102)] was obtained as a colorless solid with a molecular formula of $C_{12}H_{16}O_5$ as determined by HRESIMS along with ^{1}H, ^{13}C, and edited-HSQC NMR data (Table 1, Table 2, Fig. S7), establishing an index of hydrogen deficiency of 5. The NMR data suggested that **6** was an α-pyrone analogue of **1**. A key difference was replacement of the allylic methylene moiety (δ_H/δ_C 2.40/32.5, dd, J = 6.4, 1.8 for H_2-6/C-6) in **1** by an oxymethine in **6** (δ_H/δ_C 4.21/66.6, dddd, J = 7.9, 2.9, 2.3, 1.7 for H-6/C-6). These data, along with a 16 amu difference in the HRMS data of compounds **1** and **6**, indicated hydroxylation at the C-6 position in **6**. The coupling constant ($J_{H\text{-}6/H\text{-}7}$ = 7.9 Hz) implied a pseudoaxial/pseudoequatorial *cis* orientation in **6** (Table 1, Fig. S7). NOESY correlations observed between H-6 and H-7 indicated that these two protons were on the same face (Fig. 4). An HMBC correlation was observed from 11-OCH_3 to C-4, indicating the connectivity of the methoxy group (Fig. 5). HMBC correlations from H-3 to C-4, C-4a, and C-2, from H_2-5 to C-6a and C-7, from H-6 to C-4a and C-8, from H-7 to C-9, and from H_3-10 to C-8 were observed (Fig. 5). The trivial name 6-hydroxy-7-*epi*-phomopsinone A was ascribed to compound **6**. The absolute configuration of **6** was assigned via a modified Mosher's ester method,[22] establishing the configurations as 6*S* and 7*R* (Fig. 2C), which were opposite to that reported for the known phomopsinone D.[10] Moreover, 6-hydroxy-7-*epi*-phomopsinone A (**6**) and phomopsinone D showed opposite CD spectra (Table S1, Fig. 3).

The specific rotation data for phomopsinone D have not been reported in the literature previously.

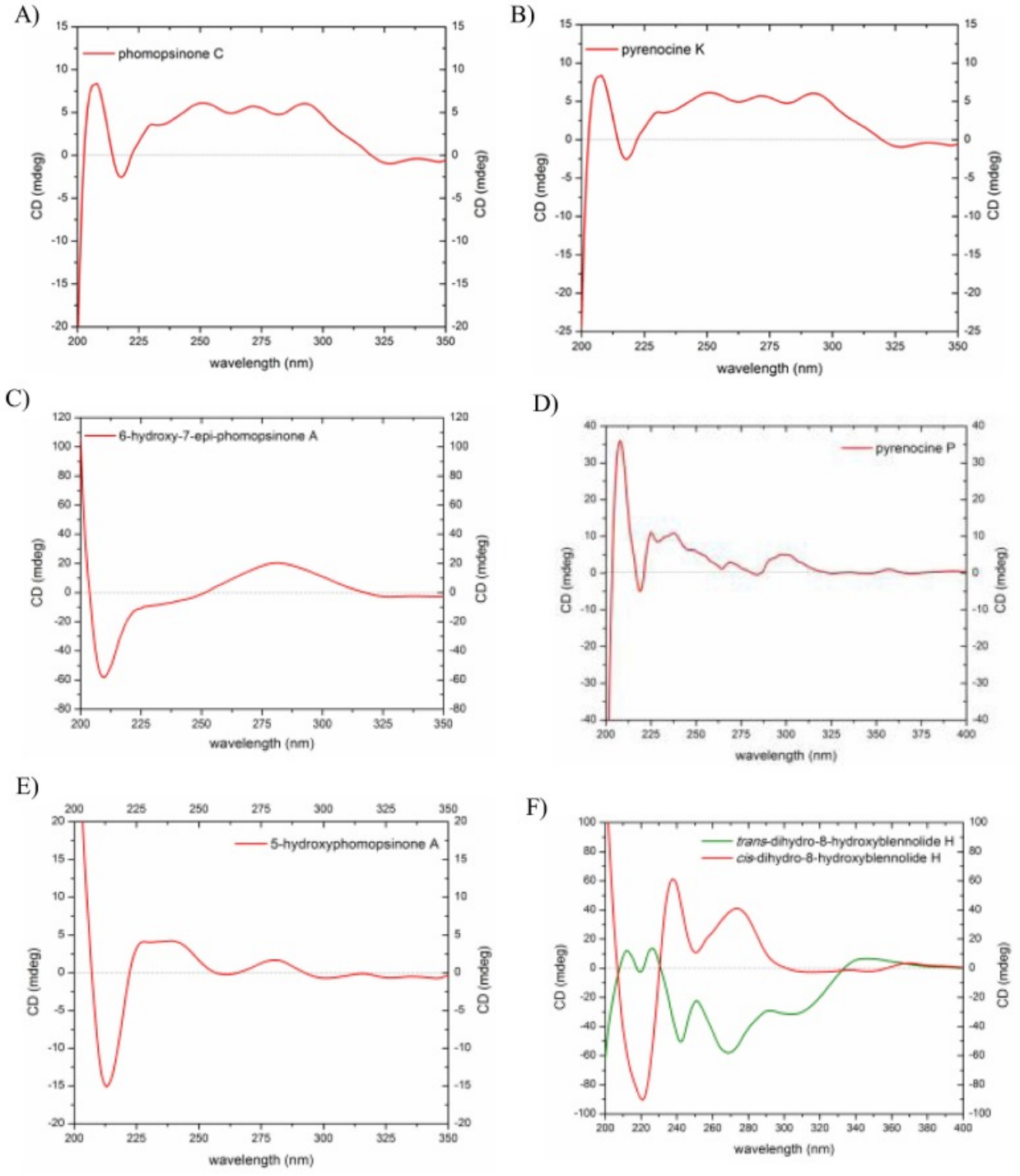

Fig. 3. ECD spectra of A) phomopsinone C (**3**) [0.58 mM] in CH_3CN; B) pyrenocine K (**5**) [0.25 mM] in CH_3OH; C) 6-hydroxy-7-*epi*-phomopsinone A (**6**) [0.12 mM] in CH_3CN; D) pyrenocine P (**8**) [0.28 mM] in CH_3OH; E) 5-hydroxyphomopsinone A (**12**) [0.13 mM] in CH_3CN, and F) *cis*-dihydro-8-hydroxyblennolide H (**15**) [0.19 mM] and *trans*-dihydro-8-hydroxyblennolide H (**16**) [0.22 mM] in $CHCl_3$, cell length 2 cm.

Table 1. ^{1}H NMR Data (700 MHz) for **5** and (500 MHz) for **6**, **8**, and **12** in $CDCl_3$.[a]

Position	5	6	8	12
3	5.43, s	5.48, s	5.45, s	5.44, s
5	4.33, dt (14.9, 2.9)	4.38, dd (15.5, 2.3)	4.38, dtd (14.9, 2.9, 0.6)	5.87, d (4.0)
	4.52, dd (14.9, 1.2)	4.51, dd (15.5, 1.7)	4.63, ddd (14.9, 1.7, 0.6)	
6	2.47, m	4.21, dddd (7.9, 2.9, 2.3, 1.7)	2.38, dt (17.2, 2.9)	2.44, m
	2.52, m		2.62, m	
7	4.12, m	3.48, ddd (8.7, 7.9, 2.9)	3.79, m	4.31, m
8	2.60, dd (17.0, 4.7)	1.55, m	3.66, m	1.57, m
	2.85, dd (17.0, 7.3)	1.82, m	3.79, m	1.64, m
9		1.43, m	3.81, s	1.42, m
		1.58, m		1.49, m
10	2.20, s	0.95, t (7.5)		0.95, t (7.5)
11	3.79, s	3.82, s		3.84, s
5-OH				2.81, d (4.0)
6-OH		2.68, d (2.9)		
8-OH			2.04, t (6.3)	

[a]δ in ppm, mult (J in Hz).

Table 2. ^{13}C NMR Data for **5** and **10** (175 MHz) and for **6**–**9**, **11**–**12** (125 MHz) in $CDCl_3$.[a]

Position	5	6	7	8	9	10	11	12
2	164.2	163.8	164.6	164.1	164.3	165.4	164.1	163.8
3	88.3	88.9	88.1	88.2	88.6	102.0	89.3	88.4
4	168.5	168.2	171.0	168.4	170.1	165.9	170.8	168.6
4a	107.6	109.1	108.9	107.6	113.7	92.9	108.6	108.9
5	61.9	61.4	9.71	61.9	54.2	8.8	9.1	87.4
6	32.3	66.6	38.9	28.3	38.5	71.4	59.3	32.6
6a	155.9	155.9	158.2	155.9	161.9	165.0	157.0	160.1
7	70.2	78.8	69.8	74.4	69.2	35.5	56.5	66.2
8	48.9	34.3	39.5	64.9	40.0	27.4		37.2
9	205.7	18.7	18.9	56.2	18.9	22.6		18.6
10	31.2	14.1	14.1		14.1	14.2		14.05
11	56.3	56.4	56.2		56.6	56.6		56.5

[a]δ in ppm.

Compound **7** [1.7 mg (G100); 0.7 mg (G102)] was obtained as a colorless solid with a molecular formula of $C_{12}H_{18}O_4$ as determined by HRESIMS along with ^{1}H, ^{13}C, and edited-HSQC NMR data (Table 2, Table 3, Fig. S8), indicating an index of hydrogen deficiency of 4. These NMR data suggested another α-pyrone analogue with structural similarities to **1**. However, a critical difference was replacement of the allylic oxymethylene moiety (δ_H/δ_C4.28/4.53/61.6, dt, J = 14.7, 2.8 and d, J = 14.7 for H-5a/H-5b/C-5) in **1** by a singlet methyl group in **7** (δ_H/δ_C 1.90/9.71). These data, along with a 2 amu difference in the HRMS data of compounds **1** and **7** and a decrease in hydrogen deficiency, indicated a cleavage of the 3,6-dihydropyran ring in **7** relative to **1**. HMBC correlations were observed from H_3-5 to C-4 and C-6a, from H_2-6 to C-4a, C-6a, and C-8, from H_3-10 to C-8, from 11-OCH_3 to C-4, and from H-3 to C-4 and C-4a (Fig. 5). The trivial name 5-deoxy-7-hydroxypyrenocine M was ascribed to compound **7**, and the absolute configuration was assigned as 7*R* via a modified Mosher's ester method[22] (Fig. 2).

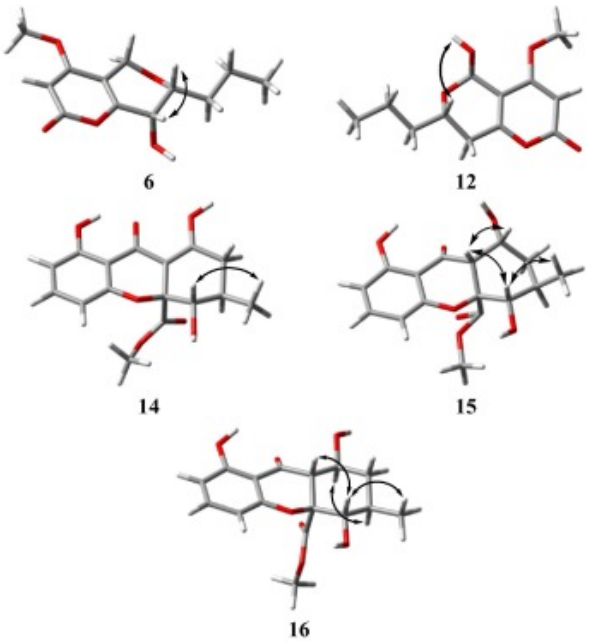

Fig. 4. Key NOESY correlations of **6**, **12**, and **14**–**16**.

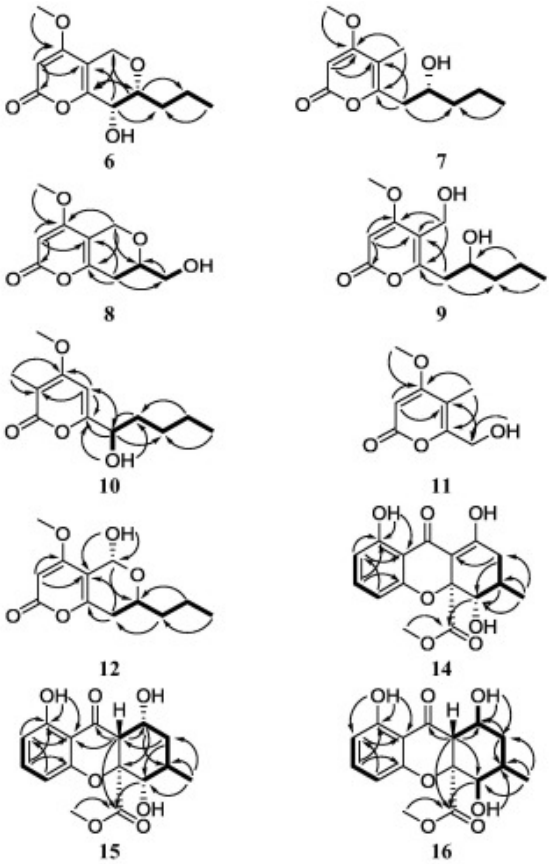

Fig. 5. Key COSY and HMBC correlations of compounds **6**–**12** and **14**–**16**.

Table 3. ^{1}H NMR Data (500 MHz) for **7** and **9**–**11** in $CDCl_3$.[a]

Position	7	9	10	11
3	5.46, s	5.47, s		5.50, s
4a			6.34, s	
5	1.90, s	4.30, d (12.6)	1.90, s	1.93, s
		4.51, d (12.6)		
6	2.62, dd (14.3, 4.0)	2.63, dd (14.3, 2.9)	4.42, m	4.46, d (6.3)
	2.69, dd (14.3, 8.6)	2.75, dd (14.3, 9.7)		
7	4.07, m	4.01, m	1.70, m	3.83, s
			1.87, m	
8	1.50, m	1.53, m	1.36, m	
			1.42, m	
9	1.38, m	1.39, m	1.34, m	
	1.50, m	1.46, m		
10	0.93, t (6.9)	0.94, t (7.5)	0.89, t (6.9)	
11	3.81, s	3.85, s	3.90, s	
5-OH		3.29, br.		
6-OH			2.02, d (5.7)	2.22, t (6.3)
7-OH		2.46, br.		

[a]δ in ppm, mult (*J* in Hz).

Compound **8** [2.5 mg (G100); 2.4 mg (G102)] was obtained as a colorless solid with a molecular formula of $C_{10}H_{12}O_5$ as determined by HRESIMS along with ^{1}H, ^{13}C, and edited-HSQC NMR data (Table 1, Table 2, Fig. S9), establishing an index of hydrogen deficiency of 5. These NMR data suggested **8** as an α-pyrone derivative with structural similarity to **1**. Key differences were observed in the aliphatic side chain, where the terminal ethyl moiety in **1** was replaced by a hydroxy group in **8**. These considerations, along with the COSY and HMBC data, established the structure of **8** (Fig. 5), which was confirmed via single crystal X-ray diffraction (Fig. 6); ECD data suggested the absolute configuration as 7*S*. The trivial name pyrenocine P was ascribed to compound **8**.

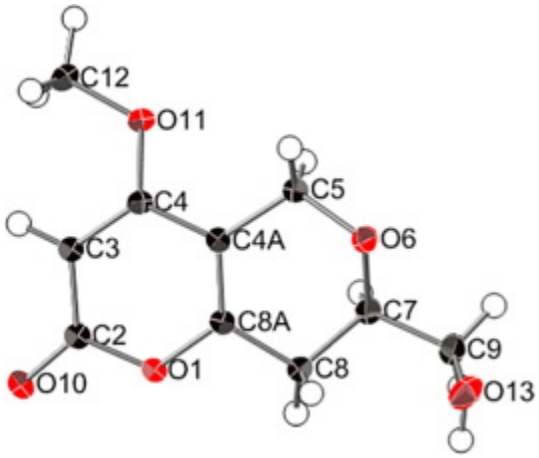

Fig. 6. X-ray crystallographic structure of **8**.

Compound **9** [6.9 mg (G102)], which was also obtained as a colorless solid, was found to have a molecular formula of $C_{12}H_{18}O_5$ as determined by HRESIMS along with ^{1}H, ^{13}C, and edited-HSQC NMR data (Table 2, Table 3, Fig. S10A), establishing an index of hydrogen deficiency of

4. The structure of **9** was determined as an α-pyrone derivative by comparison of its NMR and HRMS data with those of **4**. A key difference was replacement of the methylene moiety (δ_H/δ_C 1.68/27.9, m, H_2-7/C-7) in **4** by an oxymethine in **9** (δ_H/δ_C4.01/69.2, m, for H-7/C-7). These data, along with a 16 amu difference in the HRMS data of compounds **4** and **9**, indicated hydroxylation at C-7 in **9**. HMBC correlations from H-3 to C-4, C-4a, and C-2, from H_2-5 to C-6a and C-4, from H_2-6 to C-4a and C-8, from H_2-9 to C-7, and from H_3-10 to C-8 were observed (Fig. 5). The trivial name 7-hyrdoxypyrenocine M was ascribed to compound **9**. In an attempt to determine the absolute configuration of **9** via a modified Mosher's ester method,[22] the compound was found to be racemic, suggesting that it may be an artifact of the purification processes (Fig. S10B).

Compound **10** [0.7 mg (G102)] was obtained as a colorless solid with a molecular formula of $C_{12}H_{18}O_4$ as determined by HRESIMS and analysis of ^{1}H, ^{13}C, and edited-HSQC NMR data (Table 2, Table 3, Fig. S11). Inspection of the NMR data suggested compound **10** as an α-pyrone analogue with structural similarity to **7**, both sharing the same molecular formula. However, the allylic methyl singlet (δ_H/δ_C 1.90/9.71, s, for H_3-5/C-5) in **7** was replaced by an olefinic proton (δ_H/δ_C 6.34/92.9, s, for H-4a/C-4a) in **10**, and the olefinic proton (δ_H/δ_C 5.46/88.1, s, for H-3/C-3) in **7** was replaced by an allylic methyl singlet (δ_H/δ_C1.90/8.8, s, for H_3-5/C-5) in **10**. These data indicated that the olefinic proton and the methyl group switched positions, which was confirmed by observed HMBC correlations from H-4a to C-6 and C-6a (Fig. 5). Another key difference included a 1,2-hydroxy shift in **10** relative to **7**. The allylic methylene moiety ($\delta_H/\delta_H/\delta_C$ 2.62/2.69/38.9, dd, J = 14.3, 4.0 and J = 14.3, 8.6, for H-6a/H-6b/C-6, respectively) in **7** was replaced by an allylic carbinol carbon (δ_H/δ_C4.42/71.4, m, for H-6/C-6), while the carbinol carbon (δ_H/δ_C 4.07/69.8, m, for H-7/C-7) in **7**was replaced by a methylene moiety ($\delta_H/\delta_H/\delta_C$ 1.70/1.87/35.5, m, for H-7a/H-7b/C-7). This shift was confirmed by the observed HMBC correlations from 6-OH to C-6a and C-7, from H_2-9 to C-7, and from H-6 to C-8 (Fig. 5). Further examination of the NMR data, including COSY and HMBC spectra (Fig. 5), yielded the structure of **10**, which was ascribed the trivial name pyrenocine Q. As for **9**, an attempt to determine the absolute configuration of **10** via a modified Mosher's ester method[22] revealed a racemic mixture of the *R* and *S*enantiomers.

Compound **11** [0.5 mg (G102)] was isolated as a colorless solid with a molecular formula of $C_8H_{10}O_4$ as revealed by analysis of the HRESIMS, ^{1}H NMR, ^{13}C NMR and edited-HSQC NMR data (Table 2, Table 3, Fig. S12), indicating an index of hydrogen deficiency of four. Inspection of the NMR data indicated **11** was a relatively simple α-pyrone derivative, but with differences in the aliphatic side chain and the 3,6-dihydropyran ring. In addition to key NMR resonances for the α-pyrone ring, NMR data indicated the presence of a methoxy group, an allylic methyl singlet and an allylic hydroxymethyl group (Table 2, Table 3, Fig. S12). These data suggested a trisubstituted *α*-pyrone derivative. HMBC correlations from H_2-6 to C-4a, from H_3-5 to C-6a, from H_3-7 to C-4, and from H-3 to C-4a confirmed the substituents' positions (Fig. 5). Further examination of the NMR data yielded the structure of **11**, which was ascribed the trivial name pyrenocine R.

Compound **12** [0.9 mg (G102)], which was isolated as a colorless solid, had a molecular formula of $C_{12}H_{16}O_5$ as deduced from HRESIMS along with ^{1}H NMR, ^{13}C NMR, and edited-HSQC NMR data (Table 1, Table 3, Fig. S13), indicating an index of hydrogen deficiency of 5.

Analysis of the NMR data indicated **12** as an α-pyrone derivative with structural similarity to **1**. A key difference was replacement of the allylic oxymethylene moiety ($\delta_H/\delta_H/\delta_C$ 4.30/4.57/61.7, dt, J = 14.9, 2.9; d, J = 14.9, for H-5a/H-5b/C-5) in **1** by a dioxymethine group in **12** (δ_H/δ_C 5.87/87.4, d, J = 4.0, for H-5/C-5). These data, along with a 16 amu difference in the HRMS data of compounds **1** and **6**, indicated hydroxylation at the C-5 position in **12**, which was further confirmed by observation of an NMR signal for the -OH group (δ_H 2.81, d, J = 4.0) that showed diagnostic HMBC correlations with C-5 and C-4a (Table 3, Fig. 5). Further analysis of the NMR spectra, including COSY and HMBC data, yielded the structure of **12**, which was given the trivial name 5-hydroxyphomopsinone A. The similarity of the ECD data of **12** (Fig. 3) with that of **1** (Fig. S2), along with the observed NOESY correlation from 5-OH to H-7, were used to establish the absolute configuration as 5*R* and 7*S* (Fig. 4).

2.2. Monomeric/dimeric tetra/hexahydroxanthones

Compounds **13**–**16** were identified as a homodimeric tetrahydroxanthone (**13**), a monomeric tetrahydroxanthone (**14**), and a pair of monomeric hexahydroxanthones (**15**–**16**). Analysis of HRMS, NMR, and ECD data identified **13** [7.4 mg (G102)] as the known secalonic acid A (Figs. S2 and S14).[17, 23] Structurally related monomeric/dimeric tetrahydroxanthones, including **13**, were isolated previously in our lab from an organic extract of the filamentous fungal culture *Setophoma terrestris*.[17]

Table 4. ^{1}H (500 MHz) and ^{13}C NMR (125 MHz) for **14** and **16**, and (100 MHz) for **15**.[a]

Position	**14**		**15**		**16**	
	δ_C	δ_H	δ_C	δ_H	δ_C	δ_H
1	162.2		162.1		162.0	
2	110.9	6.52, d (8.0)	110.5	6.53, d (8.0)	110.7	6.53, d (8.6)
3	138.3	7.35, dd (8.6, 8.0)	139.0	7.40, t (8.0)	139.2	7.40, dd (8.6, 8.0)
4	108.1	6.55, d (8.6)	107.7	6.59, d (8.0)	107.9	6.54, d (8.0)
4a	159.0		160.3		159.7	
5	77.1	3.90, d (10.9)	78.1	3.52, d (10.9)	79.2	3.76, dd (10.9, 3.4)
6	29.4	2.40, m	28.5	2.26, m	31.7	1.84, m
7	36.4	2.29, dd (19.5, 10.9)	39.7	1.53, ddd (14.3, 12.6, 2.9)	39.0	1.27, dd (13.2, 11.5)
		2.72, dd (19.5, 6.3)		2.02, dt (14.3, 3.4)		2.13, ddd (13.2, 5.2, 4.0)
8	177.7		67.9	4.37, d (4.0)	66.0	4.82, m
8a	101.8		52.4	3.12, d (4.0)	56.2	2.94, d (9.2)
9	187.2		196.9		199.0	
9a	107.2		109.8		107.7	
10a	84.9		85.0		87.8	
11	18.2	1.15, d (6.3)	17.9	1.15, d (6.9)	18.3	1.11, d (6.3)
12	170.5		171.1		169.3	
13	53.4	3.68, s	53.6	3.67, s	53.3	3.62, s
1-OH		11.23, s		11.58, s		11.12, s
5-OH		2.77, br.				2.67, d (3.4)
8-OH						3.64, d (1.7)

[a]δ in ppm, mult (J in Hz).

Compound **14** [2.3 mg (G102)] was obtained as a colorless solid with a molecular formula of $C_{16}H_{16}O_6$ deduced by HRESIMS and analysis of ^{1}H NMR, ^{13}C NMR and edited-HSQC NMR data (Table 4, Fig. S15), indicating an index of hydrogen deficiency of 9. Analysis of the HRMS

and NMR data suggested **14** as a tetrahydroxanthone derivative with structural similarity to the monomeric units of **13**. However, a key difference was replacement of the C-2 quaternary carbon in **13** (δ_C 118.3) by an aromatic methine in **14** (δ_H/δ_C 6.52/110.9, d, J = 8.0). COSY data identified two spin systems as H-2/H-3/H-4 and H-5/H-6/H_2-7 (Fig. 5). Further examination of the NMR spectra, including HMBC data (Fig. 5), yielded the gross structure of **14**, which was identical to the monomeric units of **13**. A NOESY correlation was observed between 11-CH_3 and H-5, indicating that those protons were on the same side of the molecule (Fig. 4). A proton doublet corresponding to H-5 (δ_H 3.90, d, J = 10.9 Hz) implied a pseudodiaxial *trans* orientation of H-5/H-6, as observed in the monomeric units of **13**.[17] These data along with biogenetic considerations established the relative configuration of **14** to be (5*S*,6*R*,10a*S*), the same as that of the monomeric units of **13**. Due to the structural similarity of **14** with blennolide H, a tetrahydroxanthone derivative that has been recently isolated in our lab,[17] compound **14** was ascribed the trivial name 8-hydroxyblennolide H. Moreover, compound **14** and blennolide H showed similar ECD spectra (Fig. S2), confirming the assignment of absolute configuration. Compound **14** was reported recently by synthesis and was described using the name (−)-blennolide B.[24] (−)-Blennolide B is an enantiomer of the natural blennolide B (which is dextro rotatory).[25] Due to this confusion with the trivial name, and because this is the first isolation of the natural product, we believe that 10-hydroxyblennolide H is a more appropriate and understandable name.

2.3. Cyclodepsipeptides

In addition to compounds **1**–**16**, two known cyclodepsipeptides, Sch 378161 (**17**) [4.6 mg (G100); 1.4 mg (G102)] and Sch 217048 (**18**) [10.7 mg (G100); 1.6 mg (G102)], were isolated and identified by means of NMR and HRMS and MS/MS data (Fig. S18), all of which compared favorably to the literature.[18, 26]

2.4. Antimicrobial activity

Compounds **1** and **4**–**18** were tested for antimicrobial activity against an array of bacteria and fungi (*Staphylococcus aureus*, *Escherichia coli, Mycobacterium smegmatis*, *Candida albicans*, and *Aspergillus niger*), but were found inactive. Compounds **1**, **2**, **6**, **8**, **13**, **14**, and **15** showed varying degrees of *in vitro* inhibition against bacterial Pth1 from several species. All but the most potent inhibitor lead to a decreased solubility of the enzyme under the conditions tested. A cloudiness in the reaction appeared upon addition of these compounds and was determined to be insoluble Pth1 from coomassie gel of the pelleted material after centrifugation. The degree of Pth1 aggregation was somewhat correlated to the amount of compound added, but also was effected by speed of compound addition, concentration of compound addition, temperature of the reaction, and was partially reversible over the course of the assay. Thus, while these compounds do appear to interact with Pth1, no meaningful quantitation of inhibition was possible. The most potent inhibitor was **13**, demonstrating an IC_{50} of 1.4 mM against *Salmonella typhimurium* Pth1 (Fig. 7). From chemical shift perturbation mapping, **13** was confirmed to bind in the active site (Fig. 8). Helping to explain the low affinity, **13** also bound to at least one other site on Pth1, in part the same secondary site which did not affect enzyme activity for a previously reported synthetic inhibitor.[20] While not promising for clinical application, these findings represent the first reported small molecule natural product inhibitor of bacterial Pth1, which to date has been

limited to crude natural product extracts.[27, 28] Therefore these compounds provide tools to expand our understanding of Pth1 inhibition. With the tremendous structural biology knowledge of apo Pth1, having an inhibitor enables an array of follow-up structure-function studies, far out weighing the lack of potency. Of particular interest is high resolution structural characterization of an inhibitor bound complex, providing understanding of small molecule Pth1 inhibition, for which there is no substrate or inhibitor bound complex known to date. Also, having inhibitors with known structures provides a means to help bridge the gap between computational docking and empirical inhibition.[29]

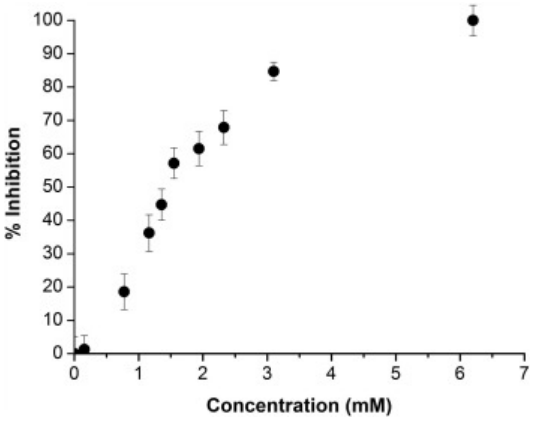

Fig. 7. Concentration-% inhibition curve of compound **13** against bacterial peptidyl-tRNA hydrolase (Pth1).

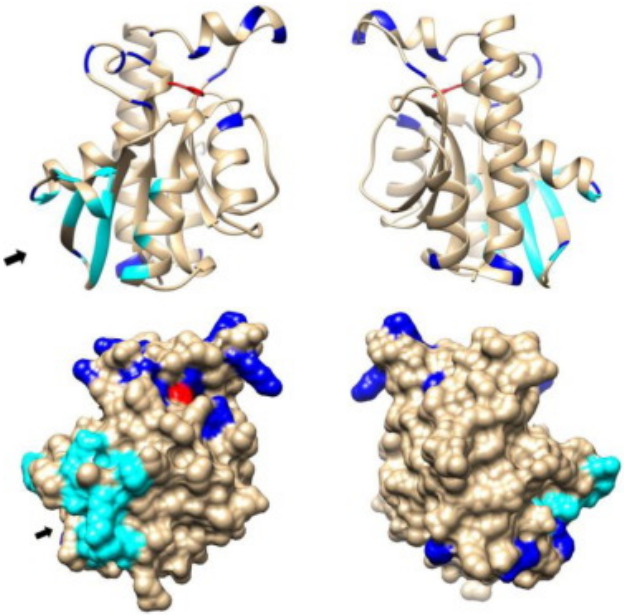

Fig. 8. ^{1}H-^{15}N Chemical shift perturbations caused by **13** (secalonic acid A) binding to *E. coli* Pth1. At top, the ribbon diagram of *E. coli* Pth1 indicates residues with chemical shift perturbations between one third and one peak width in cyan and those greater than the peak width in blue. Catalytically essential His20 is red, with the side chain in the active site cleft shown. Below, the corresponding surface representations of Pth1 are colored as in part A. The cluster of perturbed residues (black arrow) indicate an interaction distinct from the Pth1 active site.

3. Conclusions

From two fungal cultures that were isolated from submerged wood in a lake, 18 compounds (**1**–**18**) belonging to three structural classes, α-pyrone, tetra/hexahydroxanthones, and cyclodepsipeptides, were isolated and characterized. The studied fungi, G100 and G102, shared the ability to biosynthesize two classes of natural products, α-pyrone and cyclodepsipeptides. On the other hand, G102 has the additional biosynthetic capabilities to generate tetrahydroxanthone derivatives. The absolute configuration of the known (**2** and **3**) and the new (**6** and **7**) α-pyrone derivatives were assigned via a modified Mosher's ester method. The relative configurations of the tetra/hexahydroxanthones (**14**–**16**) were determined through NOE data. Via testing these compounds against a new assay for inhibition of bacterial Pth1,[30] the first natural product inhibitor (**13**) for this potential antibiotic target was identified. While target based screening for antibacterials has many well documented challenges,[31] identification of Pth1 inhibitors opens the possibility for characterization of an inhibitor bound complex, which may, in turn, lead to more meaningful use of computational aspects aimed at inhibitor design/development. Interestingly, the dimeric tetrahydroxantione class of compounds, such as **13**, seems to be attracting interest of the synthetic community.[24] The current study is another demonstration[4] that understudied biodiversity, regardless of its proximity to urban vs rural vs extreme locations, often reveals new chemical diversity.

4. Experimental

4.1. General experimental procedures

Optical rotations, UV data, and ECD spectra were obtained using a Rudolph Research Autopol III polarimeter (Rudolph Research Analytical), a Varian Cary 100 Bio UV–vis spectrophotometer (Varian Inc.), and an Olis DSM 17 ECD spectrophotometer (Olis, Inc.). NMR data were collected using either a JEOL ECA-500 NMR spectrometer operating at 500 MHz for ^{1}H and 125 MHz for ^{13}C, or a JEOL ECS-400 NMR spectrometer operating at 400 MHz for ^{1}H and 100 MHz for ^{13}C and equipped with a high sensitivity JEOL Royal probe and a 24-slot autosampler (both from JEOL Ltd.), or an Agilent 700 MHz NMR spectrometer (Agilent Technologies), equipped with a cryoprope, operating at 700 MHz for ^{1}H and 175 MHz for ^{13}C. Residual solvent signals were utilized for referencing. HRMS utilized a Thermo LTQ Orbitrap XL mass spectrometer equipped with an electrospray ionization source (Thermo Fisher Scientific). A Waters Acquity UPLC system (Waters Corp.) utilizing a Waters BEH C_{18} column (1.7 μm; 50 × 2.1 mm) was used to evaluate the purity of the isolated compounds with data collected and analyzed using Empower 3 software. Phenomenex Gemini-NX C_{18} analytical (5 μm; 250 × 4.6 mm), preparative (5 μm; 250 × 21.2 mm), and semipreparative (5 μm; 250 × 10.0 mm) columns (all from Phenomenex) were used on a Varian Prostar HPLC system equipped with ProStar 210 pumps and a Prostar 335 photodiode array detector (PDA), with data collected and analyzed using Galaxie Chromatography Workstation software (version 1.9.3.2, Varian Inc.). Flash chromatography was performed on a Teledyne ISCO CombiFlash Rf 200 using Silica Gold columns (both from Teledyne Isco) and monitored by UV and evaporative light-scattering detectors. Single crystal X-ray diffraction data were collected using a Bruker APEX CCD diffractometer (Mo Kα radiation, graphite monochromator). The crystallographic

images were generated using CrystalMaker (CrystalMaker Software). All other reagents and solvents were obtained from Fisher Scientific and were used without further purification.

4.2. Fungal strains isolation and identification

Fungal strains G100 and G102 were isolated from conidia that were found on samples of submerged wood collected from Lake Brandt (36°10′01.0″N 79°50′18.0″W) in Greensboro, North Carolina, USA in October 2011. Collecting methods and culturing conditions utilized protocols outlined previously.[32, 33, 34] Identifications were based on observation of micromorphological characters using an Olympus microscope (BX53) equipped with an Olympus DP25 camera. Molecular sequence data were obtained from internal transcribed spacer regions 1 & 2 and 5.8S nrDNA (ITS).[21] DNA extraction, PCR amplification, and sequencing were performed using previously described methods.[1, 2, 35] To obtain identification via sequence comparisons, the ITS region was BLAST searched against both GenBank and the UNITE databases.[36] Results from BLAST search suggested sequence similarities between G100 and G102 to certain taxa within the order Pleosporales, Dothideomycetes, Ascomycota. G100 showed similarity (94%) to *Clohesyomyces aquaticus*,[37, 38] whereas, G102 showed similarity (98%) to *Clohesyomyces* sp. (MAFF 239218; GenBank: JQ435791). Interestingly, G100 was also morphologically identical to *Clohesyomyces aquaticus* (Fig. S20). The sequences with high homology were downloaded and analyzed using Maximum Likelihood[39] to phylogenetically evaluate the evolutionary affinities of the two isolates (G100, and G102). Based on the results of morphology, BLAST search, and phylogenetic analysis of the ITS region, strain G100 was identified as *Clohesyomyces aquaticus*, while strain G102 was identified as having phylogenetic affinities to *Clohesyomyces* sp. (MAFF 239218; GenBank: JQ435791) (Fig. S19). The ITS sequences for both strains were deposited in the GenBank (G100: KM589855; G102: KU926856). Voucher cultures of strain G100 and G102 are maintained in the Department of Chemistry and Biochemistry culture collection at the University of North Carolina at Greensboro.

4.3. Fermentation, extraction and isolation

Extraction and fractionation of four fungal cultures of G100 and three fungal cultures of G102 grown on rice, each weighing about 25 g, were performed as described previously.[3] The organic defatted extract of G102 fungal culture (240 mg) was dissolved in $CHCl_3$, adsorbed onto Celite 545, and fractionated via normal-phase flash chromatography using a gradient solvent system of hexane–$CHCl_3$–MeOH at a 30 mL/min flow rate and 61.0 column volumes over 34.1 min to afford five fractions. Fraction 2 (103.0 mg) was subjected to preparative HPLC using a gradient system of 40:60–80:20 of CH_3CN–H_2O (0.1% formic acid) over 15 min at a flow rate of 21.24 mL/min to yield 6 sub-fractions. Sub-fractions 2 and 3 yielded compounds **1** (27.8 mg) and **14** (2.3 mg), which eluted at 11.2 min and 12.7 min, respectively. Fraction 3 (26.8 mg) was subjected to preparative HPLC using a gradient system of 30:70–80:20 of CH_3CN–H_2O (0.1% formic acid) over 30 min at a flow rate of 21.24 mL/min to yield 10 sub-fractions. Sub-fractions 1, 2, 3, 4, 5, and 7 yielded compounds **5** (0.5 mg), **15** (0.6 mg), **16** (1.3 mg), **7** (2.8 mg), **10** (0.7 mg), and **13** (7.4 mg), which eluted at 5.5 min, 6.6 min, 8.2 min, 11.0 min, 13.5 min, and 25.7 min, respectively. Compounds **7** (2.8 mg) and **16** (1.3 mg) were subjected to further purification using semipreparative HPLC using a gradient system of 40:60–60:40 of CH_3OH–

H_2O (0.1% formic acid) over 15 min at a flow rate of 4.72 mL/min to yield compounds **7** (0.7 mg) and **16** (1.0 mg), which eluted at 18.5 min and 12.6 min, respectively. Fraction 4 (37.5 mg) was subjected to preparative HPLC using a gradient system of 20:80–80:20 of CH_3CN–H_2O (0.1% formic acid) over 30 min at a flow rate of 21.24 mL/min to yield 12 sub-fractions. Sub-fractions 1, 2, 6, 7, and 8 yielded compounds **8** (2.4 mg), **11** (1.0 mg), **12** (0.9 mg), **6** (1.2 mg), and **4** (1.7 mg), which eluted at 4.3 min, 5.0 min, 13.3 min, 15.5 min, and 16.5 min, respectively. Compound **11** (1.0 mg) was subjected to further purification using semipreparative HPLC using a gradient system of 20:80 to 40:60 of CH_3OH–H_2O (0.1% formic acid) over 15 min at a flow rate of 4.72 mL/min to yield compound **11** (0.5 mg), which eluted at 13.0 min. Sub-fractions 3 (7.4 mg) and 4 (2.0 mg) were combined and subjected to preparative HPLC using an isocratic system of 20:80 of CH_3CN–H_2O (0.1% formic acid) at a flow rate of 21.24 mL/min to yield compounds **3** (0.7 mg), **9** (4.7 mg), and **2** (2.0 mg), which eluted at 43.0 min, 46.5 min, and 53.5 min, respectively. Compound **2** (2.0 mg) was subjected to further purification using semipreparative HPLC using an isocratic system of 25:75 of CH_3OH–H_2O (0.1% formic acid) at a flow rate of 4.72 mL/min to yield compound **2**(0.8 mg), which eluted at 38.0 min. Fraction 5 (63.9 mg) was subjected to preparative HPLC using a gradient system of 20:80–80:20 of CH_3CN–H_2O (0.1% formic acid) over 30 min at a flow rate of 21.24 mL/min to yield 9 sub-fractions. Sub-fractions 1, 3, and 5 yielded compounds **9** (2.2 mg), **17** (1.4 mg), and **18** (1.6 mg), which eluted at 7.9 min, 22.4 min, 24.3 min, respectively.

In an analogous manner, the organic defatted extract of G100 fungal culture (170 mg) was dissolved in $CHCl_3$, adsorbed onto Celite 545, and fractionated via normal-phase flash chromatography using a gradient solvent system of hexane–$CHCl_3$–MeOH at a 30 mL/min flow rate and 61.0 column volumes over 34.1 min to afford five fractions. Extensive preparative and semipreparative HPLC purifications of fractions 2–5 yielded compounds **1** (6.1 mg), **4** (0.8 mg), **6** (2.0 mg), **7** (1.7 mg), **8** (2.5 mg), **17** (4.6 mg), and **18** (10.7 mg).

4.3.1. Phomopsinone A (**1**)

Colorless solid; $[\alpha]_D^{24}$ = +121° (*c* = 0.18, MeOH); CD (*c* 2.23 × 10^{-4} M, CH_3CN) λ ($\Delta\varepsilon$) 287 (+14.9) nm, 264 (+10.7) nm, 237 (+10.4) nm, 210 (−49.7) nm; HRESIMS *m*/*z* 225.1118 $[M+H]^+$ (calcd for $C_{12}H_{17}O_4$ 225.1121).

4.3.2. Phomopsinone B (**2**)

Colorless solid; $[\alpha]_D^{24}$ = +28.3° (*c* = 0.09, MeOH); HRESIMS *m*/*z* 241.1070 $[M+H]^+$ (calcd for $C_{12}H_{17}O_5$ 241.1071).

4.3.3. Phomopsinone C (**3**)

Colorless solid; $[\alpha]_D^{24}$ = +42.9° (*c* = 0.06, MeOH); CD (*c* 5.83 × 10^{-4} M, CH_3CN) λ ($\Delta\varepsilon$) 294 (+7.5) nm, 271 (+6.8) nm, 250 (+7.1) nm, 214 (−13.4) nm, 207 (+16.5) nm, 200 (−24.5) nm; HRESIMS *m*/*z* 241.1070 $[M+H]^+$ (calcd for $C_{12}H_{17}O_5$ 241.1071).

4.3.4. Pyrenocine K (**5**)

Colorless solid; $[\alpha]_D^{24}$ = +43.8° (*c* = 0.05, MeOH); CD (*c* 2.52 × 10^{-4} M, CH_3OH) λ ($\Delta\varepsilon$) 300 (4.5) nm, 272 (8.5) nm, 246 (5.7) nm, 230 (12.1) nm, 223 (27.2) nm; ^{1}H NMR ($CDCl_3$, 500 MHz) and ^{13}C NMR ($CDCl_3$, 125 MHz), see Table 1, Table 2; HRESIMS *m*/*z* 239.0915 $[M+H]^+$ (calcd for $C_{12}H_{15}O_5$ 239.0914).

4.3.5. 6-Hydroxy-7-*epi*-phomopsinone A (**6**)

Colorless solid; $[\alpha]_D^{24}$ = +56.4° (*c* = 0.08, MeOH); UV (MeOH) λ_{max} (log ε) 285 (3.41), 212 (3.28) nm; CD (*c* 1.25 × 10^{-4} M, CH_3CN) λ ($\Delta\varepsilon$) 209 (−67.4) nm, 225 (−10.1) nm, 233 (−8.4) nm; 282 (+20.8) nm; ^{1}H NMR ($CDCl_3$, 500 MHz) and ^{13}C NMR ($CDCl_3$, 125 MHz), see Table 1, Table 2; HRESIMS *m*/*z* 241.1071 $[M+H]^+$ (calcd for $C_{12}H_{17}O_5$ 241.1071).

4.3.6. 5-Deoxy-7-hyrdoxypyrenocine M (**7**)

Colorless solid; $[\alpha]_D^{24}$ = −38.4° (*c* = 0.11, MeOH); UV (MeOH) λ_{max} (log ε) 285 (3.25), 212 (3.22) nm; ^{1}H NMR ($CDCl_3$, 500 MHz) and ^{13}C NMR ($CDCl_3$, 125 MHz), see Table 1, Table 2; HRESIMS *m*/*z* 227.1278 $[M+H]^+$ (calcd for $C_{12}H_{19}O_4$ 227.1278).

4.3.7. Pyrenocine P (**8**)

Colorless solid; $[\alpha]_D^{24}$ = +78.2° (*c* = 0.11, MeOH); UV (MeOH) λ_{max} (log ε) 282 (3.43), 214 (3.25) nm; ^{1}H NMR ($CDCl_3$, 500 MHz) and ^{13}C NMR ($CDCl_3$, 125 MHz), see Table 1, Table 2; HRESIMS *m*/*z* 213.0756 $[M+H]^+$ (calcd for $C_{10}H_{13}O_5$ 213.0758).

4.3.8. (±)-7-Hyrdoxypyrenocine M (**9**)

Colorless solid; UV (MeOH) λ_{max} (log ε) 283 (3.36), 213 (3.33) nm; ^{1}H NMR ($CDCl_3$, 500 MHz) and ^{13}C NMR ($CDCl_3$, 125 MHz), see Table 2, Table 3; HRESIMS *m*/*z* 243.1229 $[M+H]^+$ (calcd for $C_{12}H_{19}O_5$ 243.1227).

4.3.9. (±)-Pyrenocine Q (**10**)

Colorless solid; UV (MeOH) λ_{max} (log ε) 246 (3.25), 212 (3.08) nm; ^{1}H NMR ($CDCl_3$, 500 MHz) and ^{13}C NMR ($CDCl_3$, 175 MHz), see Table 2, Table 3; HRESIMS *m*/*z* 227.1275 $[M+H]^+$ (calcd for $C_{12}H_{19}O_4$ 227.1278).

4.3.10. Pyrenocine R (**11**)

Colorless solid; UV (MeOH) λ_{max} (log ε) 284 (2.93), 211 (3.04) nm; ^{1}H NMR ($CDCl_3$, 500 MHz) and ^{13}C NMR ($CDCl_3$, 125 MHz), see Table 2, Table 3; HRESIMS *m*/*z* 171.0650 $[M+H]^+$ (calcd for $C_8H_{11}O_4$ 171.0652).

4.3.11. 5-Hydroxyphomopsinone A (**12**)

Colorless solid; $[\alpha]_D^{24} = -4.5°$ (c = 0.07, MeOH); UV (MeOH) λ_{max} (log ε) 280 (3.45), 213 (3.28) nm; ^{1}H NMR ($CDCl_3$, 500 MHz) and ^{13}C NMR ($CDCl_3$, 125 MHz), see Table 2, Table 3; HRESIMS m/z 241.1071 $[M+H]^+$ (calcd for $C_{12}H_{17}O_5$ 241.1070).

4.3.12. 8-Hydroxyblennolide H (**14**)

Colorless solid; $[\alpha]_D^{24} = -113.3°$ (c = 0.11, MeOH); UV (MeOH) λ_{max} (log ε) 334 (3.26), 277 (3.36), 222 (3.46) nm; CD (c 1.56 × 10^{-4} M, $CHCl_3$) λ ($\Delta\varepsilon$) 379 (−14.4) nm, 328 (−23.4) nm, 293 (−19.4), 248 (−43.3), 236 (+52.1), 226 (−126.2) nm; ^{1}H NMR ($CDCl_3$, 500 MHz) and ^{13}C NMR ($CDCl_3$, 125 MHz), see Table 4; HRESIMS m/z 321.0968 $[M+H]^+$ (calcd for $C_{16}H_{17}O_7$ 321.0969).

4.3.13. *cis*-Dihydro-8-hydroxyblennolide H (**15**)

Colorless oil; $[\alpha]_D^{24} = -72.7°$ (c = 0.09, MeOH); UV (MeOH) λ_{max} (log ε) 354 (3.18), 276 (3.55), 222 (3.53) nm; CD (c 1.86 × 10^{-4} M, $CHCl_3$) λ ($\Delta\varepsilon$) 344 (−2.2) nm, 274 (+45.0) nm, 237 (+87.1) nm, 225 (−113.6) nm; ^{1}H NMR ($CDCl_3$, 500 MHz) and ^{13}C NMR ($CDCl_3$, 100 MHz), see Table 4; HRESIMS m/z 323.1117 $[M+H]^+$ (calcd for $C_{16}H_{19}O_7$ 323.1125).

4.3.14. *trans*-Dihydro-8-hydroxyblennolide H (**16**)

Colorless oil; $[\alpha]_D^{24} = +38.2°$ (c = 0.08, MeOH); UV (MeOH) λ_{max} (log ε) 349 (3.13), 272 (3.48), 222 (3.48) nm; CD (c 2.17 × 10^{-4} M, $CHCl_3$) λ ($\Delta\varepsilon$) 344 (+6.9) nm, 274 (−54.9) nm, 237 (−18.4) nm, 225 (+22.1) nm; ^{1}H NMR ($CDCl_3$, 500 MHz) and ^{13}C NMR ($CDCl_3$, 125 MHz), see Table 4; HRESIMS m/z 323.1126 $[M+H]^+$ (calcd for $C_{16}H_{19}O_7$ 323.1125).

4.3.15. Preparation of the (*R*)- and (*S*)-MTPA ester derivatives of phomopsinone B (**2**), phomopsinone C (**3**), 6-hydroxy-7-*epi*-phomopsinone A (**6**) and 5-deoxy-7-hyrdoxypyrenocine (**7**)

To 0.13, 0.15, 0.20 and 0.15 mg of compounds **2**, **3**, **6** and **7** were added 400 µL of pyridine-d_5 and transferred into NMR tubes. To initiate the reactions, 10 µL of *S*-(+)-α-methoxy-α-(trifluoromethyl)phenylacetyl (MTPA) chloride were added into each tube with careful shaking and then monitored immediately by ^{1}H NMR at the following time points 5, 10, 15, and 30 min. The reactions completed within 5, 5, 30 and 5 min, respectively, yielding the mono (*R*)-MTPA ester derivatives (**2b**) of **2**, (**3b**) of **3**, (**6b**) of **6**, and (**7b**) of **7**. ^{1}H NMR data (500 MHz, pyridine-d_5) of **2b**: δ_H 4.31 (^{1}H, d, J = 14.9, H-5a), 4.61 (1H, d, J = 14.9, H-5b), 1.83 (2H, m, H_2-8), 5.62 (1H, m, H-9), 1.30 (3H, d, J = 5.7, H_3-10); of **3b**: δ_H 4.15 (1H, d, J = 14.9, H-5a), 4.52 (1H, d, J = 14.9, H-5b), 2.08 (1H, m, H-6a), 2.33 (1H, m, H-6b), 1.75 (1H, m, H-8a), 5.52 (1H, m, H-9), 1.38 (3H, d, J = 6.3, H_3-10); of **6b**: δ_H 5.68 (1H, s, H-3), 4.32 (1H, d, J = 14.9, H-5a), 4.49 (1H, d, J = 14.9, H-5b), 5.99 (1H, d, J = 6.9, H-6), 1.45 (1H, m, H-9a), and 0.88 (3H, t, J = 7.5, H_3-10); of **7b**: 5.79 (1H, s, H-3), 1.84 (3H, s, H_3-5), 2.82 (1H, dd, J = 14.9, 5.2, H-6a), 3.03 (1H, dd, J = 14.9, 8.6, H-6b), 5.64 (1H, m, H-7), 1.60 (1H, m, H-8a), 1.69 (1H, m, H-8b), 1.23 (1H, m, H-9a), and 0.76 (3H, t, J = 7.5, H_3-10). In an analogues manner, 0.13, 0.15, 0.20 and 0.15 mg of **2**, **3**, **6** and **7** dissolved in 400 µL pyridine-d_5 were reacted in NMR tubes with 10 µL (*R*)-(−)-*a*-MTPA chloride for 30 and 5 min, respectively, to afford the mono (*S*)-MTPA esters

(**2a**, **3a**, **6a** and **7a**). ^{1}H NMR data (500 MHz, pyridine-d_5) of **2a**: δ_H 4.21 (1H, d, J = 14.9, H-5a), 4.57 (1H, d, J = 14.9, H-5b), 1.79 (2H, m, H-8), 5.60 (1H, m, H-9), 1.37 (3H, d, J = 6.3, H_3-10); of **3a**: δ_H 4.26 (1H, d, J = 14.9, H-5a), 4.57 (1H, d, J = 14.9, H-5b), 2.14 (1H, m, H-6a), 2.44 (1H, m, H-6b), 1.79 (1H, m, H-8a), 5.59 (1H, m, H-9), 1.29 (3H, d, J = 6.3, H_3-10); of **6a**: δ_H 5.74 (1H, s, H-3), 4.30 (1H, d, J = 14.9, H-5a), 4.51 (1H, d, J = 14.9, H-5b), 6.03 (1H, d, J = 6.9, H-6), 1.35 (1H, m, H-9a), and 0.83 (3H, t, J = 7.5, H_3-10); of **7b**: 5.73 (1H, s, H-3), 1.62 (3H, s, H_3-5), 2.70 (1H, dd, J = 14.9, 4.0, H-6a), 2.96 (1H, dd, J = 14.9, 8.6, H-6b), 5.66 (1H, m, H-7), 1.64 (1H, m, H-8a), 1.76 (1H, m, H-8b), 1.35 (1H, m, H-9a), and 0.83 (3H, t, J = 7.5, H_3-10).

4.4. X-ray crystallography

Crystallographic data for compound **8** has been deposited with the Cambridge Crystallographic Data Centre, deposition number CCDC 1473567. Compound's **8** crystals were grown in MeOH at rt. X-ray crystal structure analysis of **8** were as follows: formula $C_{10}H_{12}O_5$, MW = 212.20, irregular, colorless crystal, approximate dimensions 0.28 × 0.24 × 0.13 mm, a = 4.1747 (3) Å, b = 10.9965 (7) Å, c = 11.0671 (7) Å, α = 70.466 (1)°, β = 85.814 (1)°, γ = 80.816 (1)°, T = 193 K, Z = 2, triclinic $P1$, $GOF = S$ = 1.03, V = 472.57 (5) Å^3, R_{int} (5123 reflections, I > 2σ(I)) = 0.019, w$R(F^2)$ = 0.099, λ = 0.71073 Å. Crystal data, data collection, structure solution and refinement details are summarized in Table S2.

4.5. Bioassay methods

Pth1 from *Escherichia coli*, *Salmonella typhimurium* and *Pseudomonas aeruginosa* was expressed and purified as described previously.[40, 41] Inhibition was determined using established procedures.[28, 30] Briefly quantification of bulk peptidyl-tRNA cleavage to free tRNA was quantified using electrophoretic separation via acid-urea gel to determine inhibitory activity of compounds under study.

Acknowledgments

The authors from the University of North Carolina at Greensboro were supported in part by internal research and development funds. We thank the City of Greensboro for permission to collect in Lake Brandt. The high-resolution mass spectrometry data were acquired in the Triad Mass Spectrometry Laboratory at the University of North Carolina at Greensboro. The Wake Forest University X-ray Facility thanks the National Science Foundation – United States (grant CHE-0234489) for funds to purchase the X-ray instrument and computers. We thank Dr. A. Horswill of the University of Iowa for helpful discussions, and Dr. J.O. Falkinham III of the Virginia Polytechnic Institute and State University for antimicrobial testing.

A. Supplementary data

Supplementary data may be found at the end of this formatted document.

References

1. Raja HA, Oberlies NH, El-Elimat T, Miller AN, Zelski SE, Shearer CA. Mycoscience. 2013;54:353.

2. Raja HA, Oberlies NH, Figueroa M, et al. Mycologia. 2013;105:959.

3. El-Elimat T, Raja HA, Figueroa M, Falkinham III JO, Oberlies NH. Phytochemistry. 2014;104:114.

4. El-Elimat T, Raja HA, Day CS, Chen W-L, Swanson SM, Oberlies NH. J Nat Prod. 2014;77:2088.

5. Paguigan ND, Raja HA, Day CS, Oberlies NH. Phytochemistry. 2016;126:59.

6. Shearer CA, Descals E, Kohlmeyer B, et al. Biodivers Conserv. 2007;16:49.

7. Hernández-Carlos B, Gamboa-Angulo M. Phytochem Rev. 2011;10:261.

8. Dong JY, Shen KZ, Sun R. Mycosystema. 2011;30:206.

9. Hussain H, Ahmed I, Schulz B, Draeger S, Krohn K. Fitoterapia. 2012;83:523.

10. Hussain H, Krohn K, Ahmed I, et al. Eur J Org Chem. 2012;1783.

11. Bräse S, Encinas A, Keck J, Nising CF. Chem Rev. 2009;109:3903.

12. Masters K-S, Bräse S. Chem Rev. 2012;112:3717.

13. Stoll A, Renz J, Brack A. Helv Chim Acta. 1952;35:2022.

14. Kurobane I, Iwahashi S, Fukuda A. Drugs Exp Clin Res. 1987;13:339.

15. Liao G, Zhou J, Wang H, et al. Oncol Rep. 2010;23:387.

16. McPhee F, Caldera PS, Bemis GW, McDonagh AF, Kuntz ID, Craik CS. Biochem J. 1996;320:681.

17. El-Elimat T, Figueroa M, Raja HA, et al. Eur J Org Chem. 2014;2015:109.

18. Hegde VR, Puar MS, Dai P, et al. J Antibiot. 2001;54:125.

19. McFeeters RL. JSM Biotechnol Bioeng. 2013;1:1006.

20. Hames CM, McFeeters H, Holloway BW, Stanley BC, Urban SV, McFeeters LR. Int J Mol Sci. 2013;14:22741.

21. Schoch CL, Seifert KA, Huhndorf S, et al. Proc Natl Acad Sci USA. 2012;109:6241.

22. Hoye TR, Jeffrey CS, Shao F. Nat Protoc. 2007;2:2451.

23. Franck B, Gottschalk E-M, Ohnsorge U, Hüper F. Chem Ber. 1966;99:3842.

24. Qin T, Iwata T, Ransom TT, Beutler JA, Porco JA. J Am Chem Soc. 2015;137:15225.

25. Zhang W, Krohn K, Ullah Z, et al. Chem Eur J. 2008;14:4913.

26. Isaka M, Palasarn S, Komwijit S, Somrithipol S, Sommai S. Tetrahedron Lett. 2014;55:469.

27. Harris SM, McFeeters H, Ogungbe IV, et al. Nat Prod Commun. 2011;6:1421.

28. McFeeters H, Gilbert MJ, Thompson RM, Setzer WN, Cruz-Vera LR, McFeeters RL. Nat Prod Commun. 2012;7:1107.

29. Ferguson PP, Holloway BW, Setzer NW, McFeeters H, McFeeters LR. Antibiotics. 2016;5.

30. Holloway WB, McFeeters H, Powell AM, Nidadavolu GS, McFeeters RLJ. Anal Bioanal Techn. 2015;6:244.

31. Payne DJ, Gwynn MN, Holmes DJ, Pompliano DL. Nat Rev Drug Discov. 2007;6:29.

32. Shearer CA, Langsam DM, Longcore JE. Fungi in freshwater habitats. In: Mueller GF, Bills GF, Foster MS, eds. Measuring and Monitoring Biological Diversity: Standard Methods for Fungi. Washington, D.C.: Smithsonian Institution Press; 2004:513.

33. Raja HA, Shearer CA. Mycologia. 2008;100:467.

34. Raja H, Schmit J, Shearer C. Biodivers Conserv. 2009;18:419.

35. El-Elimat T, Figueroa M, Raja HA, et al. Tetrahedron Lett. 2013;54:4300.

36. Kõljalg U, Nilsson RH, Abarenkov K, et al. Mol Ecol. 2013;22:5271.

37. Zhang H, Hyde KD, McKenzie EHC, Bahkali AH, Zhou D. Cryptogam Mycol. 2012;33:333.

38. Hyde K. Aust Syst Bot. 1993;6:169.

39. Schmitt I, Barker FK. Nat Prod Rep. 2009;26:1585.

40. Vandavasi V, Taylor-Creel K, McFeeters RL, Coates L, McFeeters H. Acta Crystallogr Sect F. 2014;70:872.

41. Hughes RC, McFeeters H, Coates L, McFeeters RL. Acta Crystallogr Sect F. 2012;68:1472.

Supplementary data

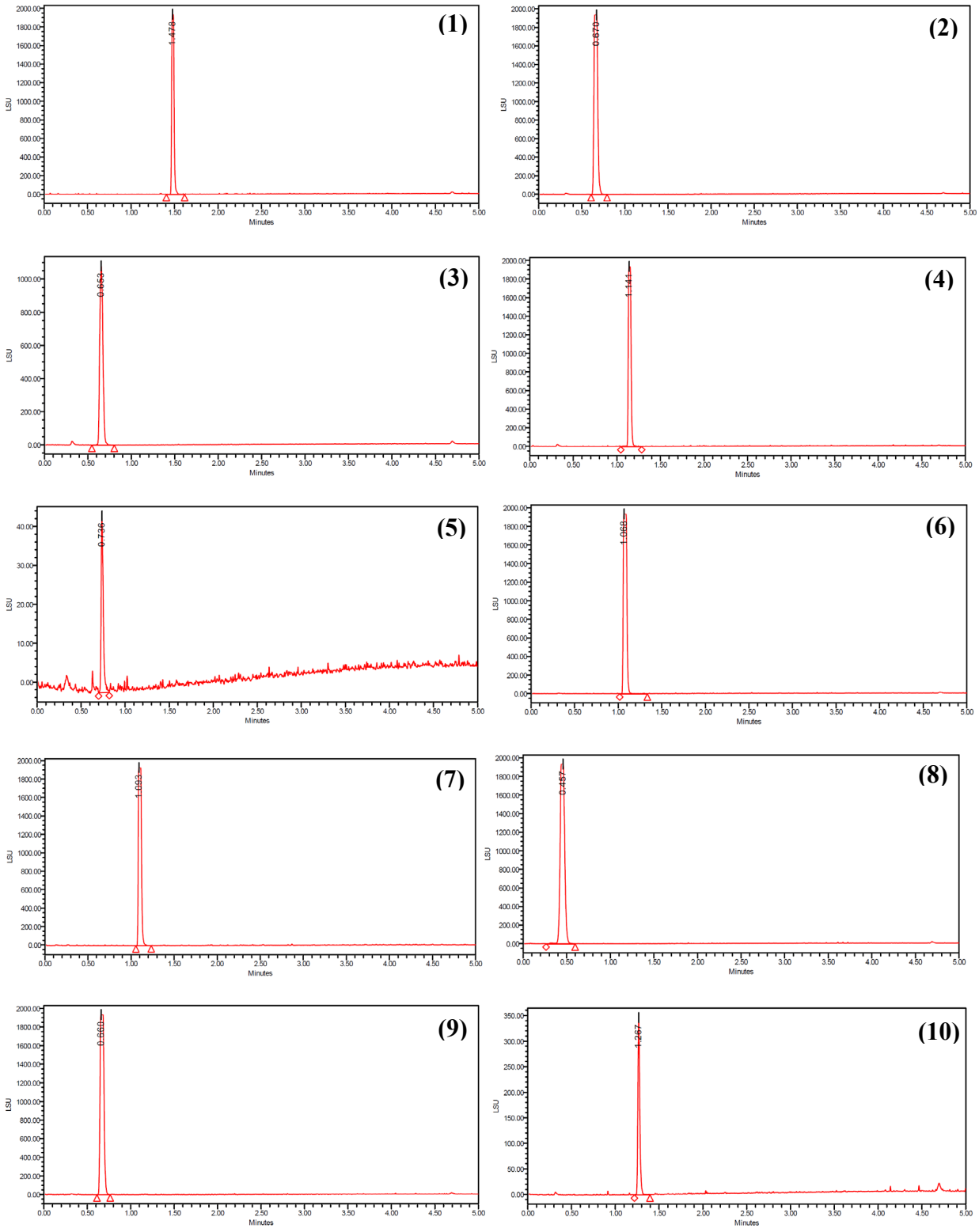

Figure S1. UPLC chromatograms of compounds **1–18** (ELSD detection), demonstarting >95% purity. All data were acquired via an Acquity UPLC system with a BEH C_{18} (1.7 μm 2.1 × 50 mm) column and a CH_3CN–H_2O gradient that incresaed linearly from 20 to 100% CH_3CN over 4.5 min.

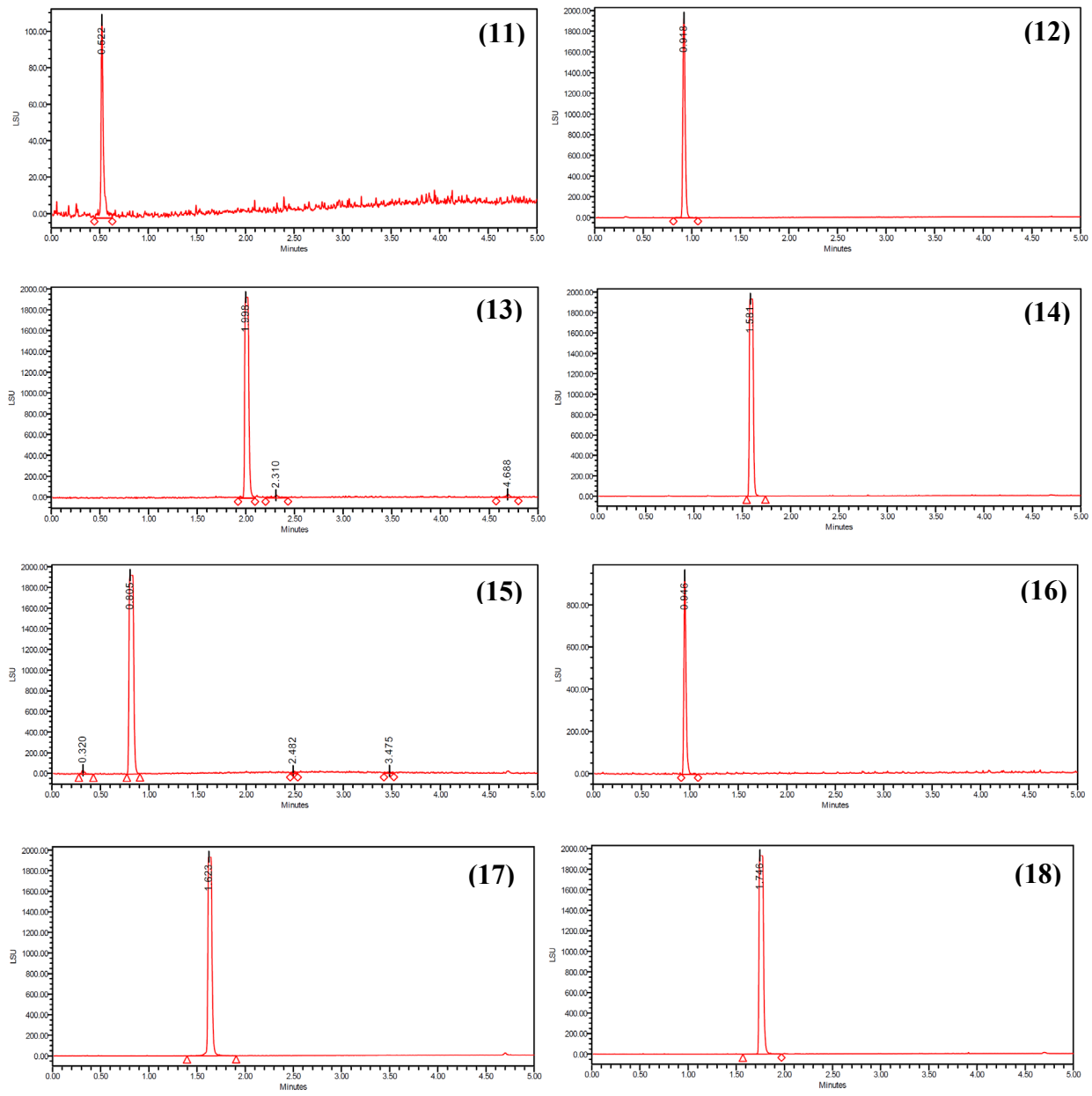

Figure S1 cont. UPLC chromatograms of compounds **1–18** (ELSD detection), demonstarting >95% purity. All data were acquired via an Acquity UPLC system with a BEH C_{18} (1.7 μm 2.1 × 50 mm) column and a CH_3CN–H_2O gradient that incresaed linearly from 20 to 100% CH_3CN over 4.5 min.

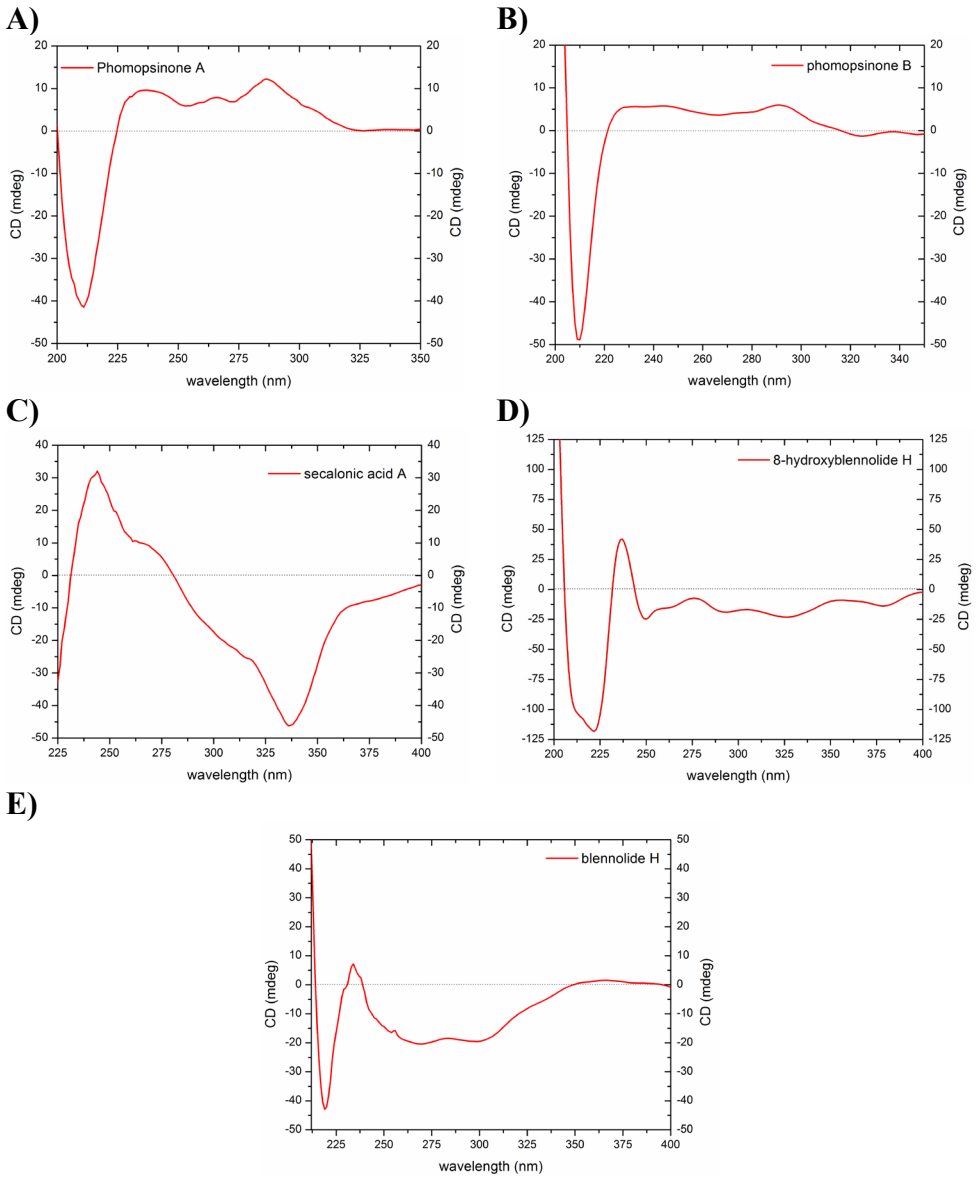

Figure S2. ECD spectra of A) phomopsinone A (**1**) [0.22 mM] in MeCN, B) phomopsinone B (**2**) [0.33 mM] in MeCN, C), and C) secalonic acid A (**13**) [0.03 mM] in $CHCl_3$, D) 8-hydroxyblennolide H (**14**) [0.16 mM] in $CHCl_3$, and E) blennolide H [0.43 mM] in MeOH, cell length 2 cm.

Table S1. CD data, experimental vs. literature, of phomopsinone A (**1**), phomopsinone B (**2**), 6-hydroxy-7-*epi*-phomopsinone A (**6**), and phomopsinone D.

Compound	CD: Conc. Solvent; λ_{max} ($\Delta\varepsilon$) nm	CD: Solvent; λ_{max} ($\Delta\varepsilon$/$M^{-1}cm^{-1}$) nm
	Experimental	**Literature**
Phomopsinone A (**1**)	2.23×10^{-4} M, CH_3CN 283 (+14.3), 264 (+10.7), 238 (+9.7), 221 (0), 213 (–48.6), 210 (–49.7), 202 (+11.8) nm	CH_3CN: λ_{max} ($\Delta\varepsilon$/$M^{-1}cm^{-1}$) = 283 (+0.48), 238 (+0.88), 223 (0), 213 (–4.17), 209 (0), 202 (+11.8) nm[a]
Phomopsinone B (**2**)	3.33×10^{-4} M, CH_3CN 387 (+6.2), 232 (+5.9), 220 (+0.7), 213 (–38.4), 209 (–62.4), 203 (+29.3) nm	CH_3CN: λ_{max} ($\Delta\varepsilon$/$M^{-1}cm^{-1}$) = 284 (+0.49), 238 (+0.48), 222 (0), 213 (–1.86), 209 (0), 201 (+5.11) nm[a]
6-hydroxy-7-epi-phomopsinone A (**6**)	1.25×10^{-4} M, CH_3CN 282 (+20.8), 251 (–0.37), 233 (–8.4), 225 (–10.1), 209 (–67.4), 202 (+28.8)	----
Phomopsinone D	-----	CH_3CN: λ_{max} ($\Delta\varepsilon$/$M^{-1}cm^{-1}$) = 283 (–1.73), 253 (0), 236 (+1.32), 216 (–0.31), 202 (+8.95), 190 (0) nm[a]

[a]Hussain, H.; Krohn, K.; Ahmed, I.; Draeger, S.; Schulz, B.; Pietro, S.; Pescitelli, G. Phomopsinones A-D: Four new pyrenocines from endophytic fungus Phomopsis sp. *Eur. J. Org. Chem.* **2012**, 1783-1789.

Table S2. NMR data for **5** and pyrenocine K (700 MHz for ^{1}H, 175 MHz for ^{13}C; chemical shifts in ppm, coupling constants in Hz, $CDCl_3$).

position	**5**		pyrenocine K[a]	
	δ_C, type	δ_H mult (*J* in Hz)	δ_C, type	δ_H mult (*J* in Hz)
2	164.2		163.9	
3	88.3	5.43, s	88.1	5.46, s
4	168.5		168.3	
4a	107.6		107.3	
5	61.9	4.33, dt (14.9, 2.9)	61.6	4.25 dd (14.5, 2.0)
		4.52, dd (14.9, 1.2)		4.53 d (14.5)
6	32.3	2.47, m	33.3	2.45 m
		2.52, m		2.55 m
6a	155.9		155.7	
7	70.2	4.12, m	69.5	4.01 m
8	48.9	2.60, dd (17.0, 4.7)	48.6	2.62 dd (14.0, 4.0)
		2.85, dd (17.0, 7.3)		2.84 dd (14.0, 4.0)
9	205.7		205.4	
10	31.2	2.20, s	32.0	2.20, s
11	56.3	3.79, s	56.0	3.81, s

[a] Hussain, H.; Ahmed, I.; Schulz, B.; Draeger, S.; Krohn, K. *Fitoterapia* 2012, 83, 523-526.

Rows highlighted in yellow show the chemical shift difference between compound **5** and those reported for pyrenocine K by Hussain et al, 2012.

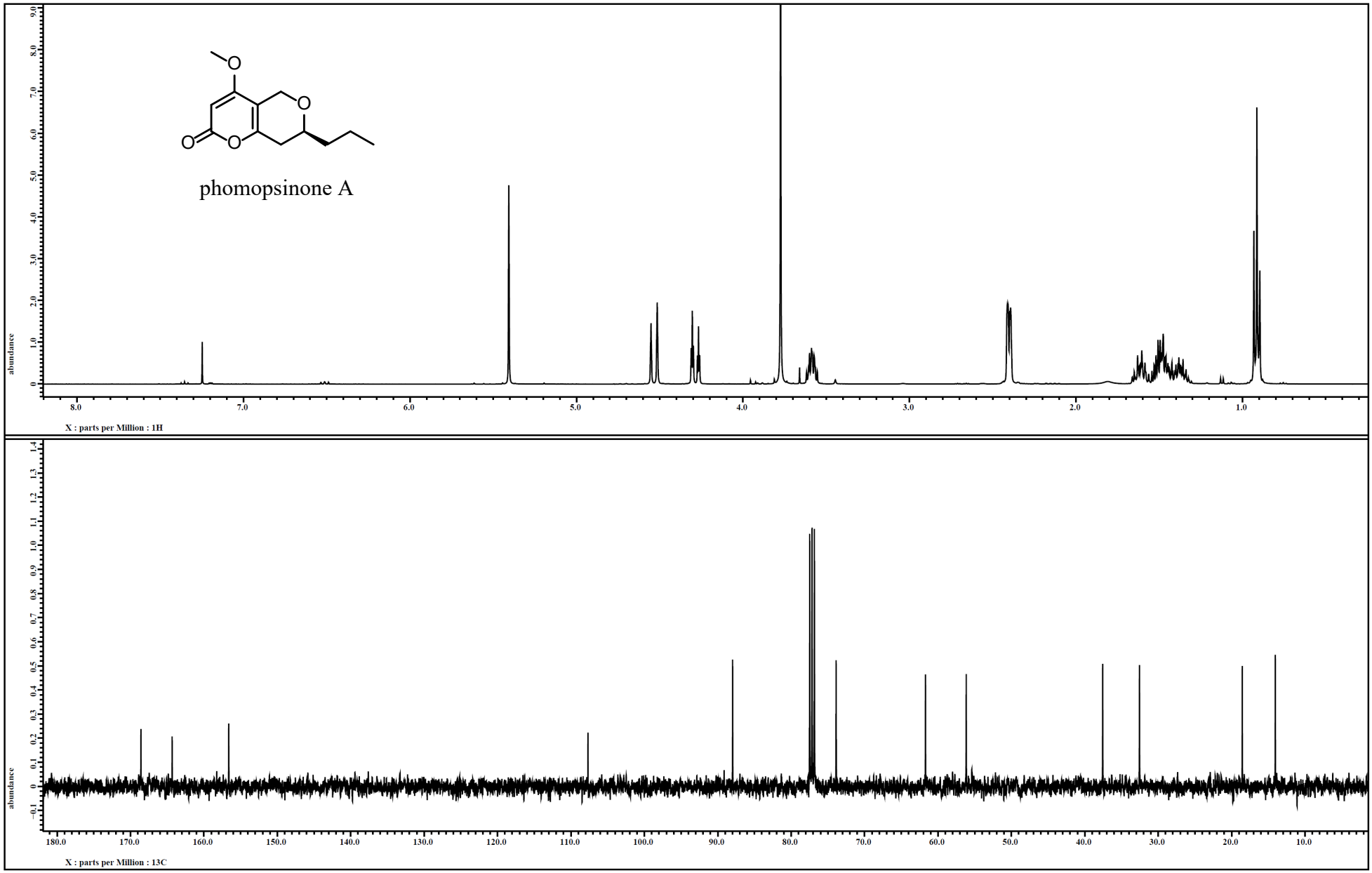

Figure S3. ^{1}H and ^{13}C NMR spectra of compound **1** [400 MHz for ^{1}H and 100 MHz for ^{13}C, $CDCl_3$].

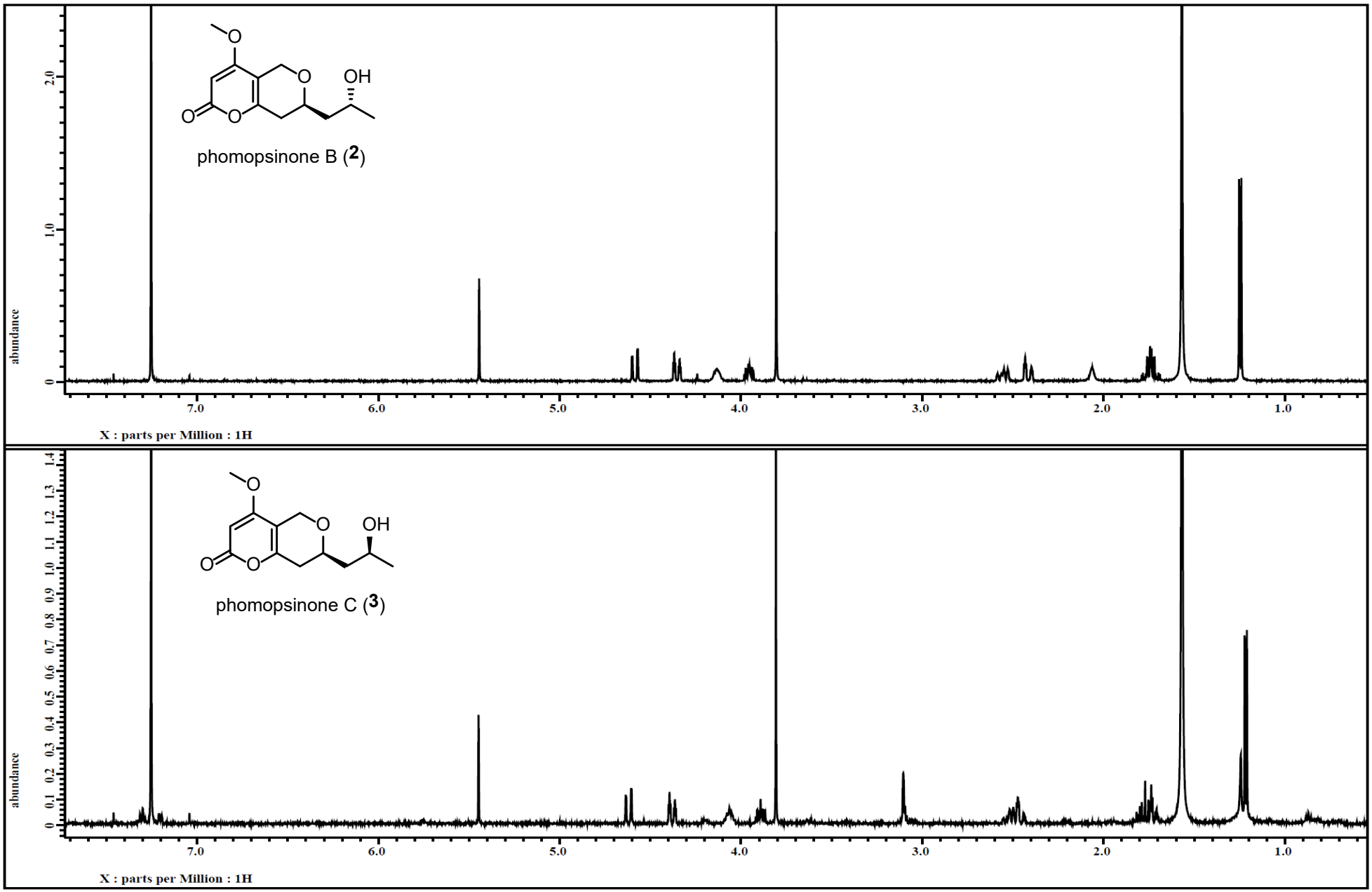

Figure S4. ^{1}H NMR spectra of compounds **2** (upper panel) and **3** (lower panel) [500 MHz, $CDCl_3$].

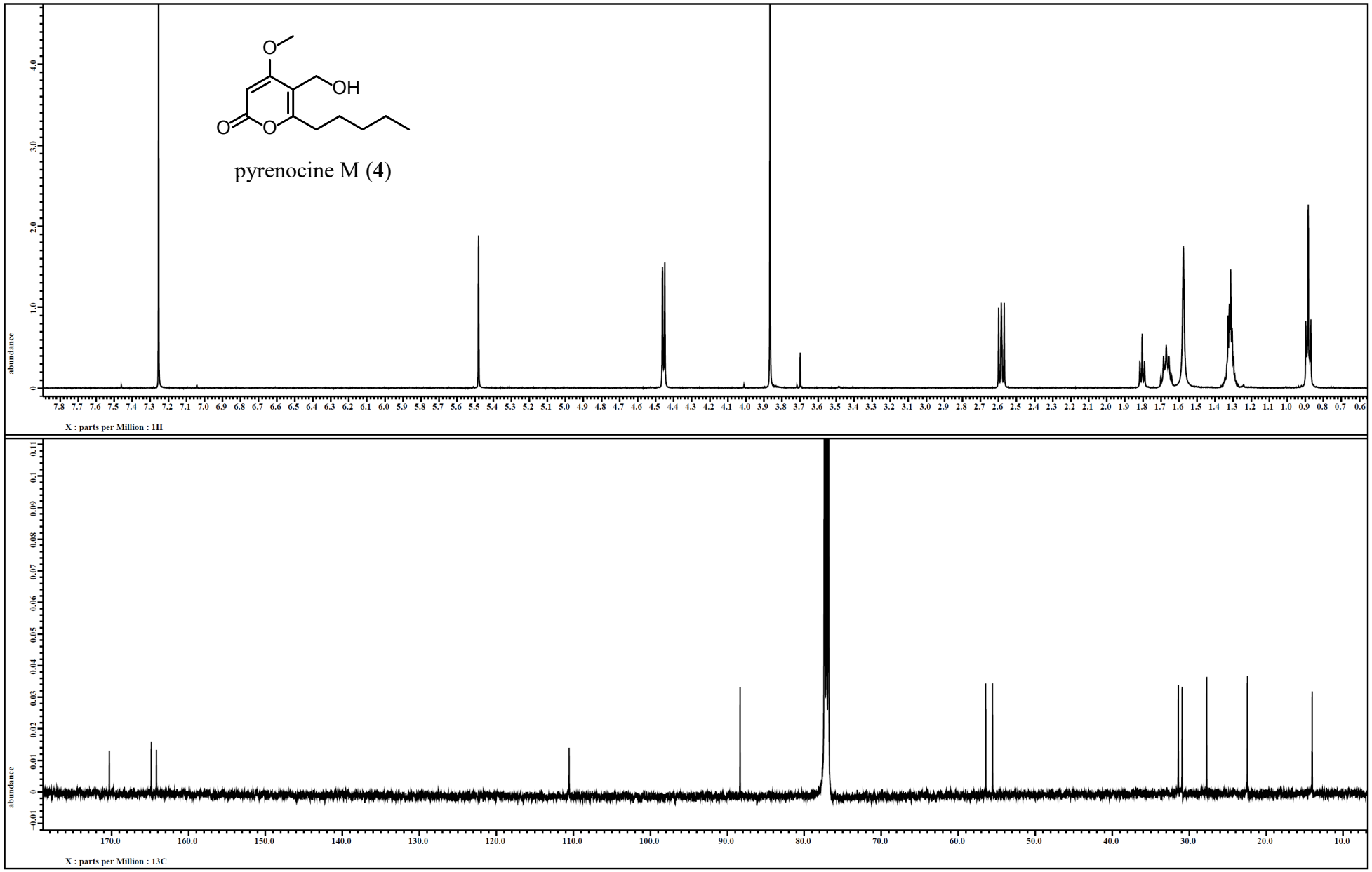

Figure S5. ^{1}H and ^{13}C NMR spectra of compound **4** [500 MHz for ^{1}H and 125 MHz for ^{13}C, $CDCl_3$].

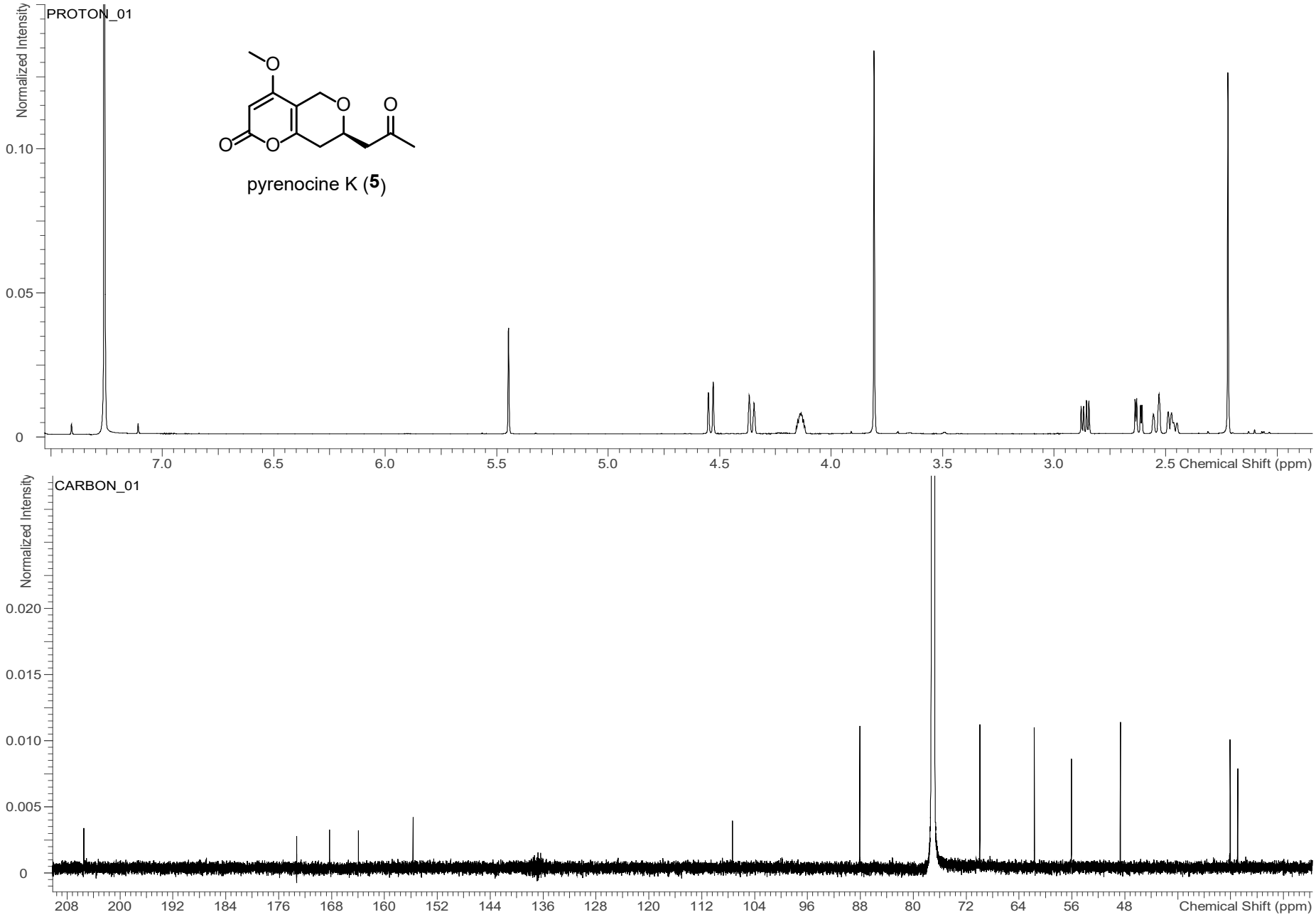

Figure S6. ^{1}H and ^{13}C NMR spectra of compound **5** [700 MHz for ^{1}H and 175 MHz for ^{13}C, $CDCl_3$].

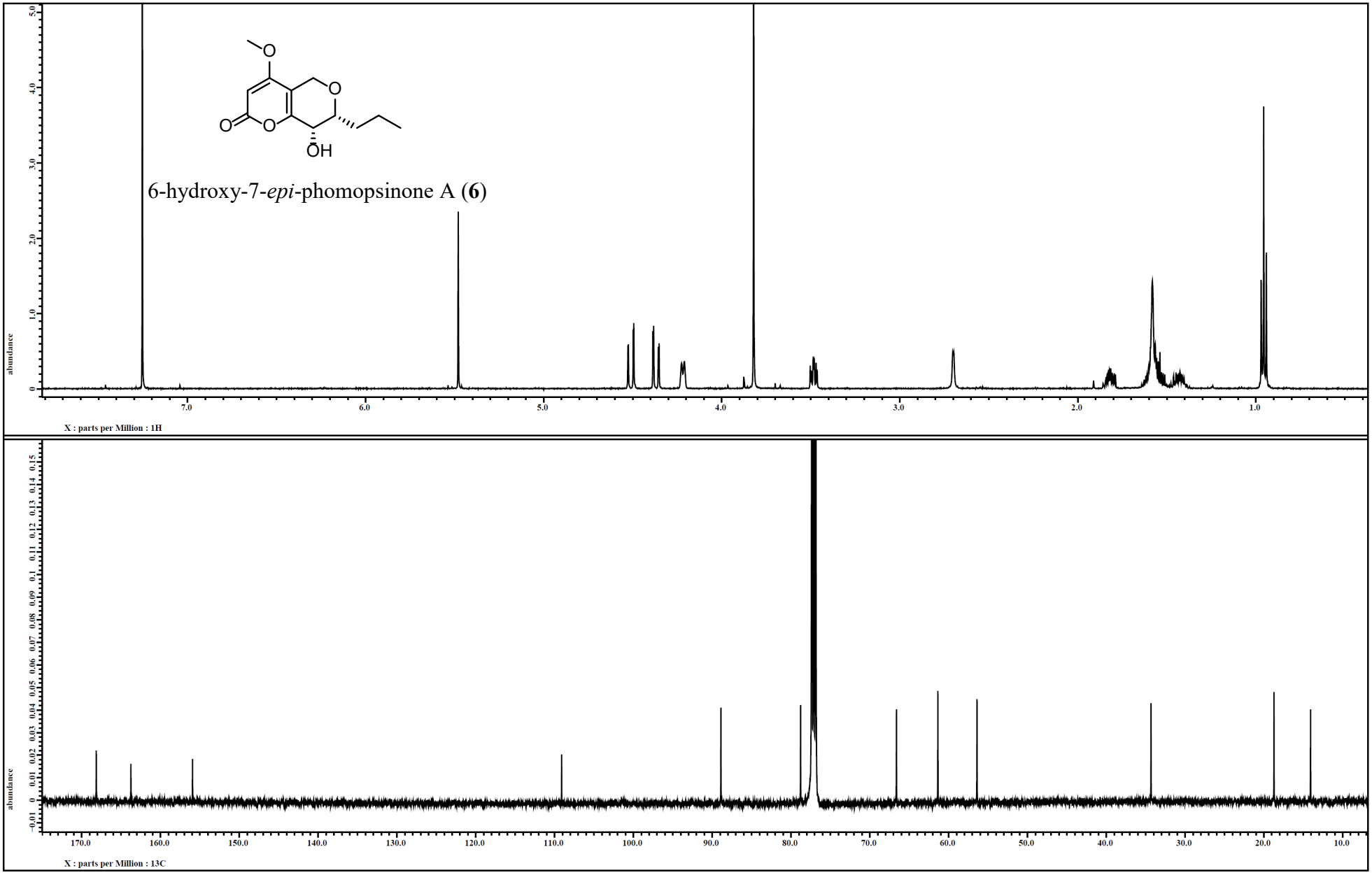

Figure S7. ^{1}H and ^{13}C NMR spectra of compound **6** [500 MHz for ^{1}H and 125 MHz for ^{13}C, $CDCl_3$].

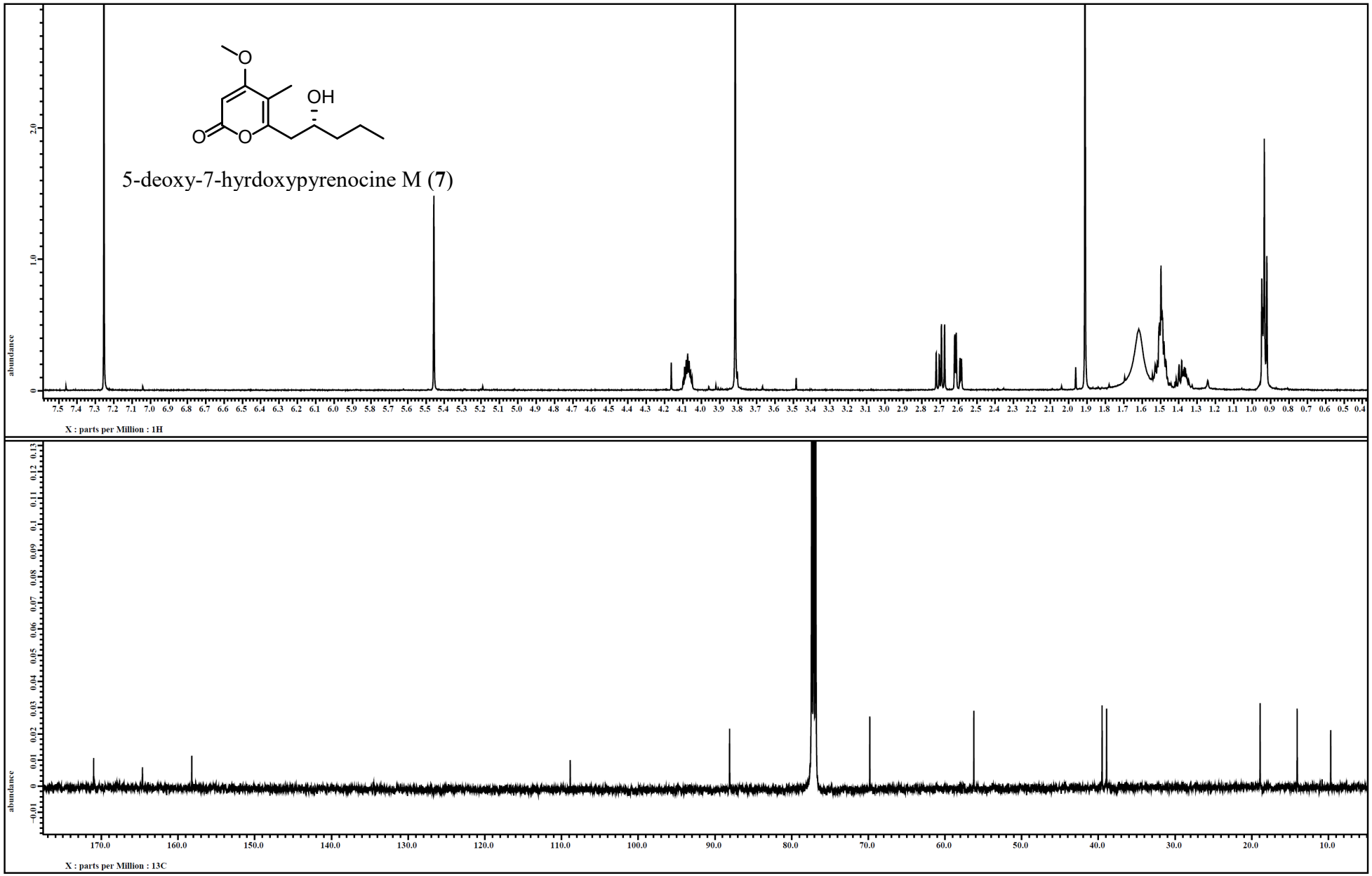

Figure S8. ^{1}H and ^{13}C NMR spectra of compound **7** [500 MHz for ^{1}H and 125 MHz for ^{13}C, $CDCl_3$].

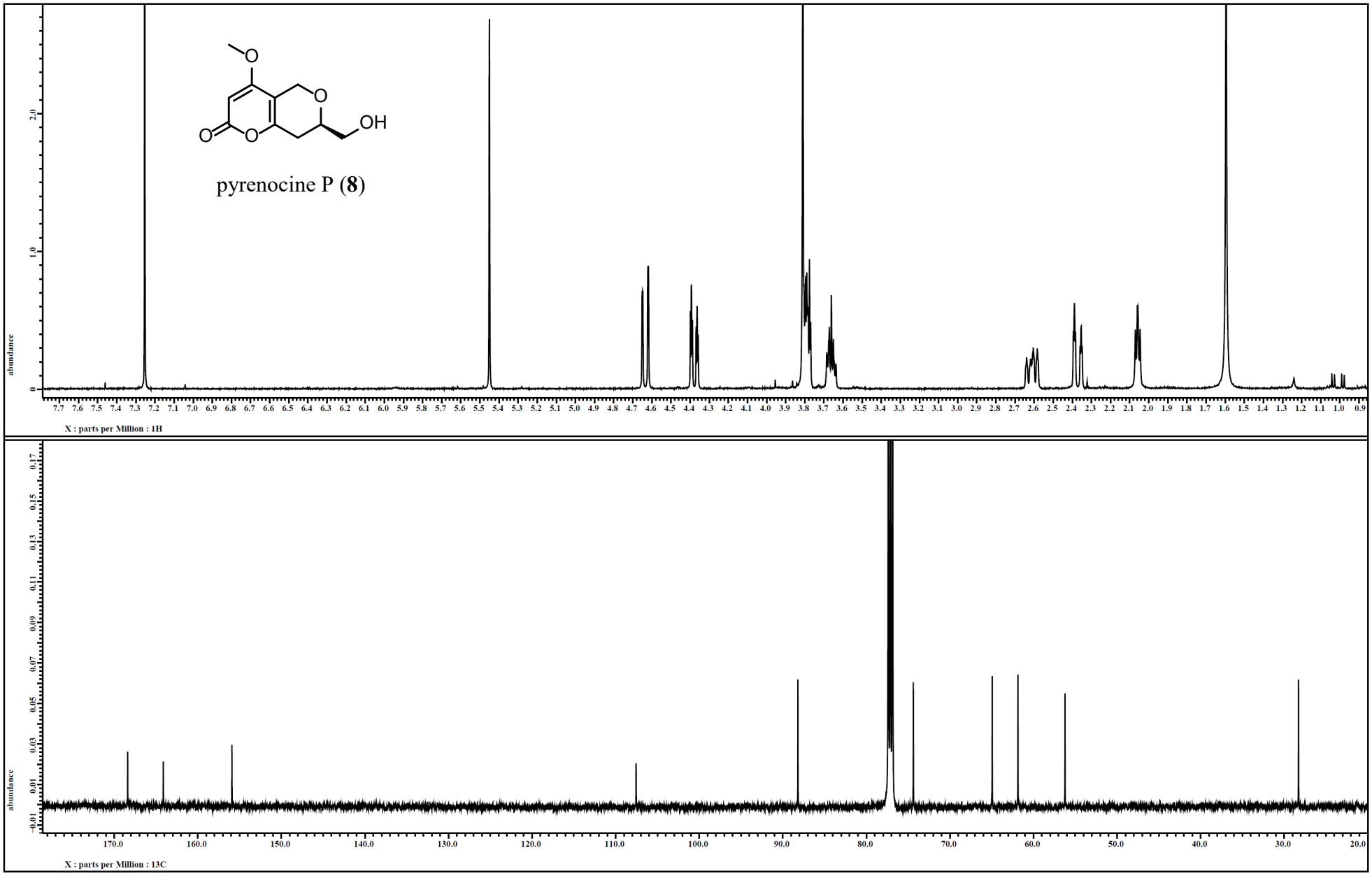

Figure S9. ^{1}H and ^{13}C NMR spectra of compound **8** [500 MHz for ^{1}H and 125 MHz for ^{13}C, $CDCl_3$].

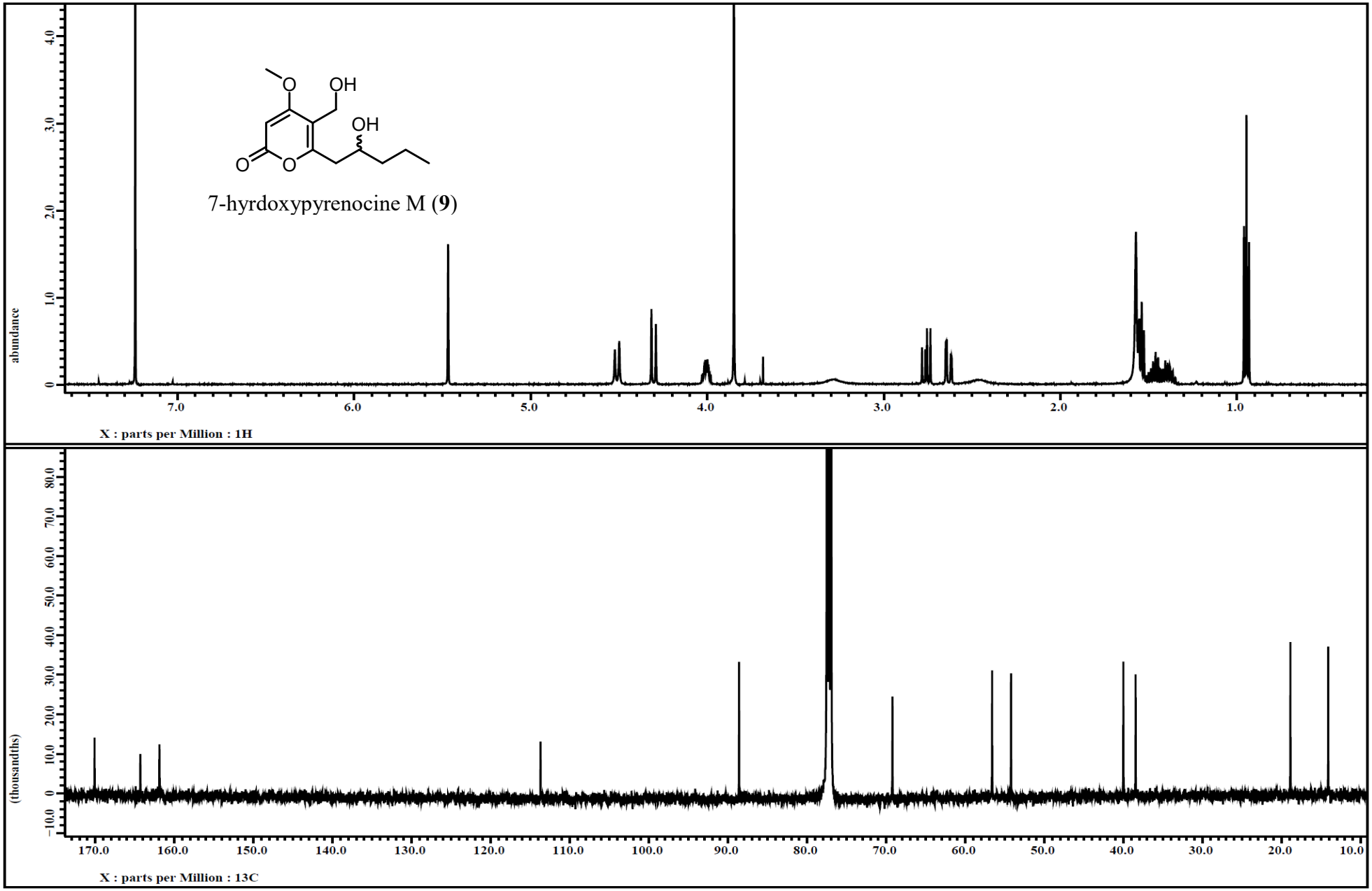

Figure S10A. ^{1}H and ^{13}C NMR spectra of compound **9** [500 MHz for ^{1}H and 125 MHz for ^{13}C, $CDCl_3$].

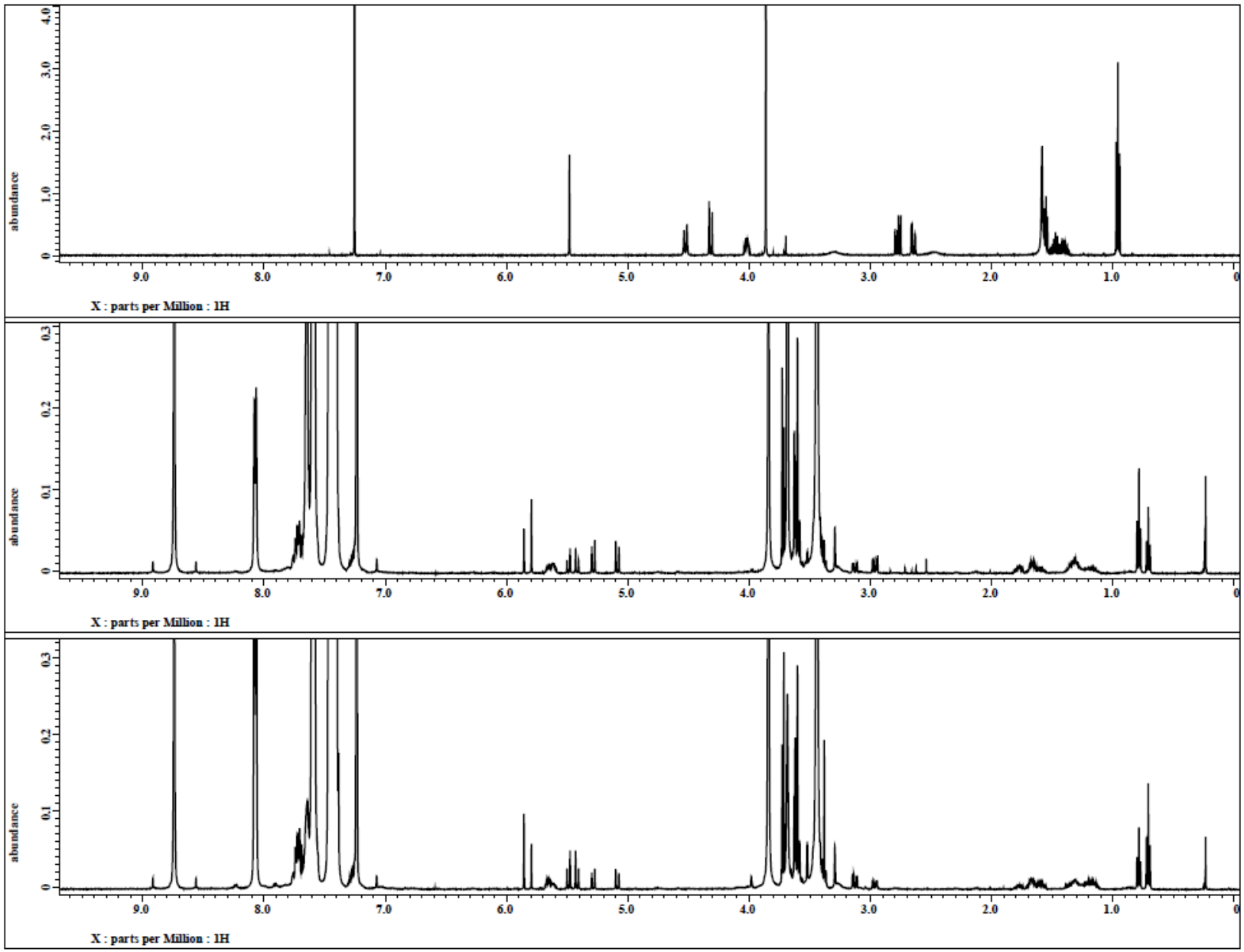
abundance
X : parts per Million : 1H
abundance
X : parts per Million : 1H
abundance
X : parts per Million : 1H

Figure S10B. [1]H NMR spectra of compound **9** (upper panel), and after reacting with *S*-(+)-*α*-methoxy-*α*-(trifluoromethyl)phenylacetyl (MTPA) chloride and (*R*)-(–)-*a*-MTPA chloride (middle and lower panels) [500 MHz, Pyridine-d_5], showing the generation of two diastereoisomers per reaction.

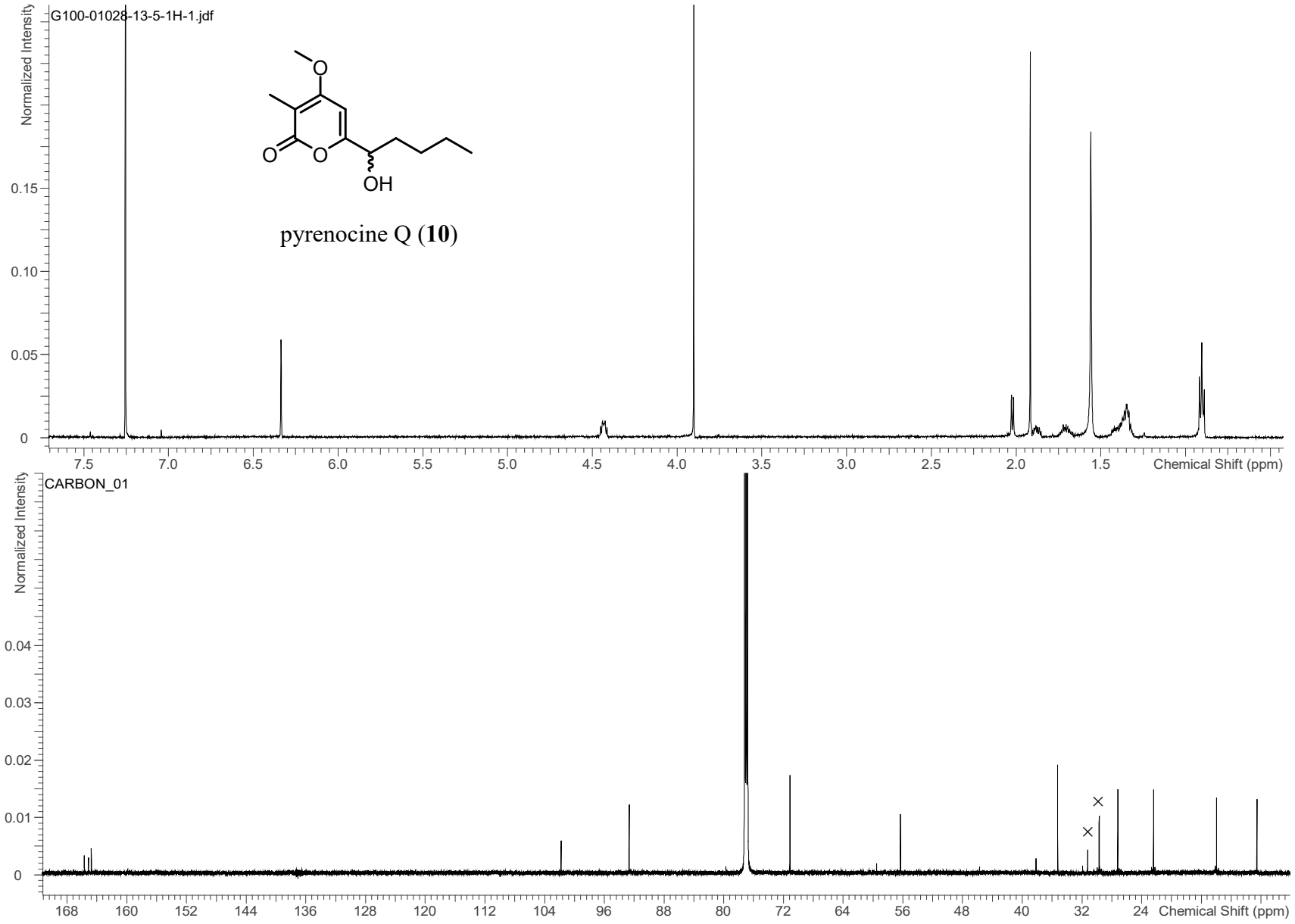

Figure S11. ^{1}H and ^{13}C NMR spectra of compound **10** [500 MHz for ^{1}H and 175 MHz for ^{13}C, $CDCl_3$].

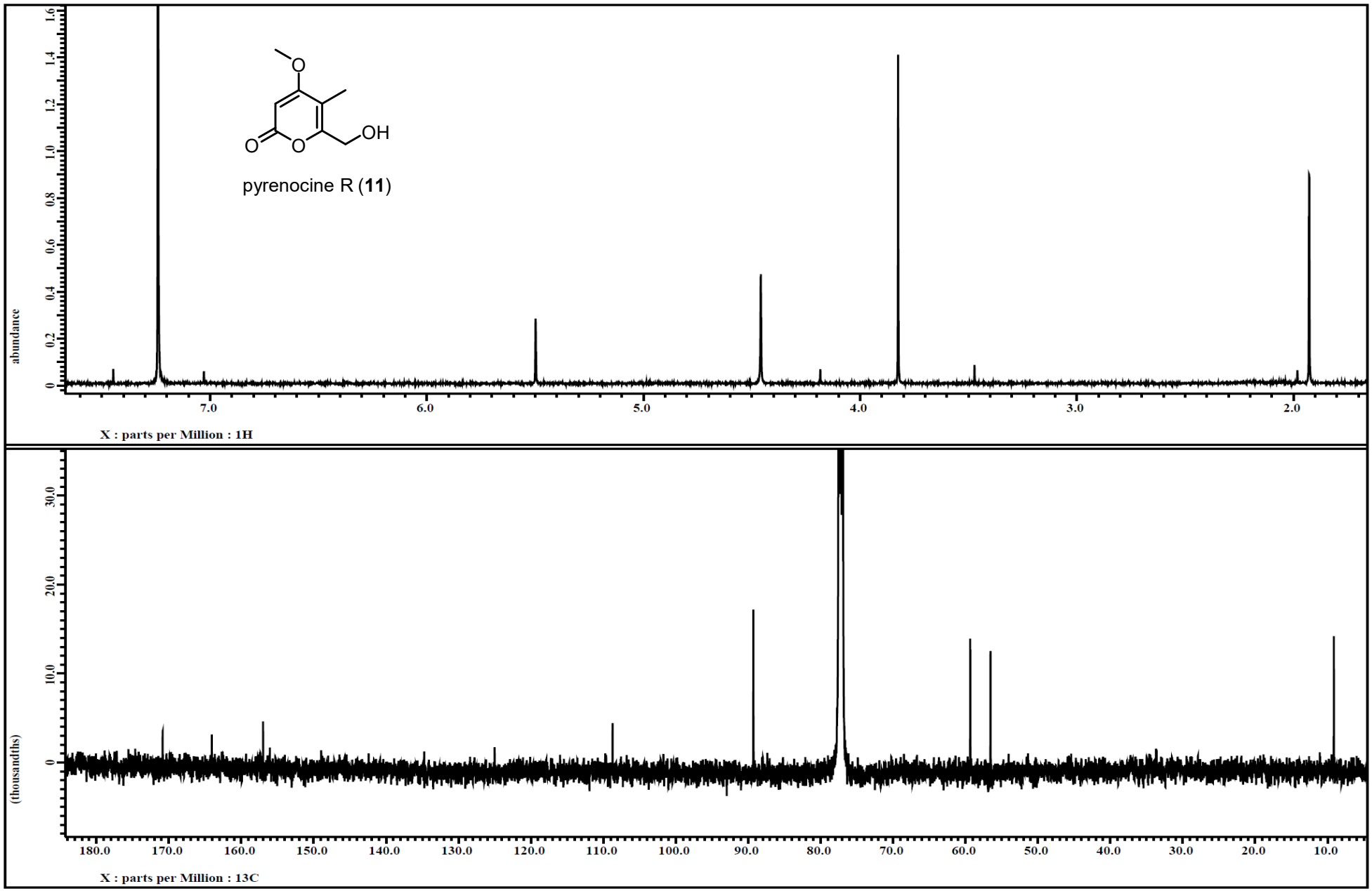

Figure S12. ^{1}H and ^{13}C NMR spectra of compound **11** [500 MHz for ^{1}H and 125 MHz for ^{13}C, $CDCl_3$].

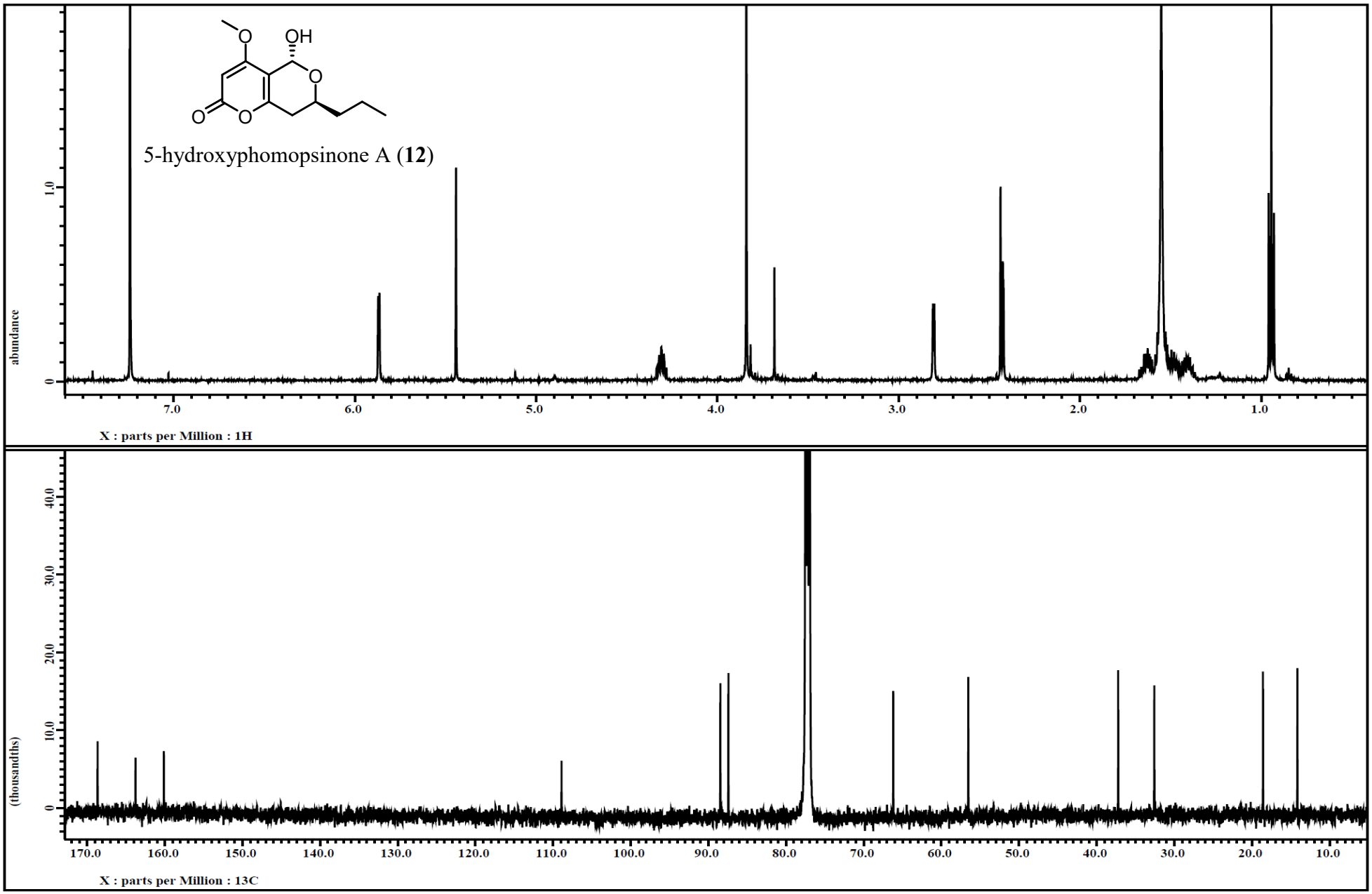

Figure S13. ^{1}H and ^{13}C NMR spectra of compound **12** [500 MHz for ^{1}H and 125 MHz for ^{13}C, $CDCl_3$].

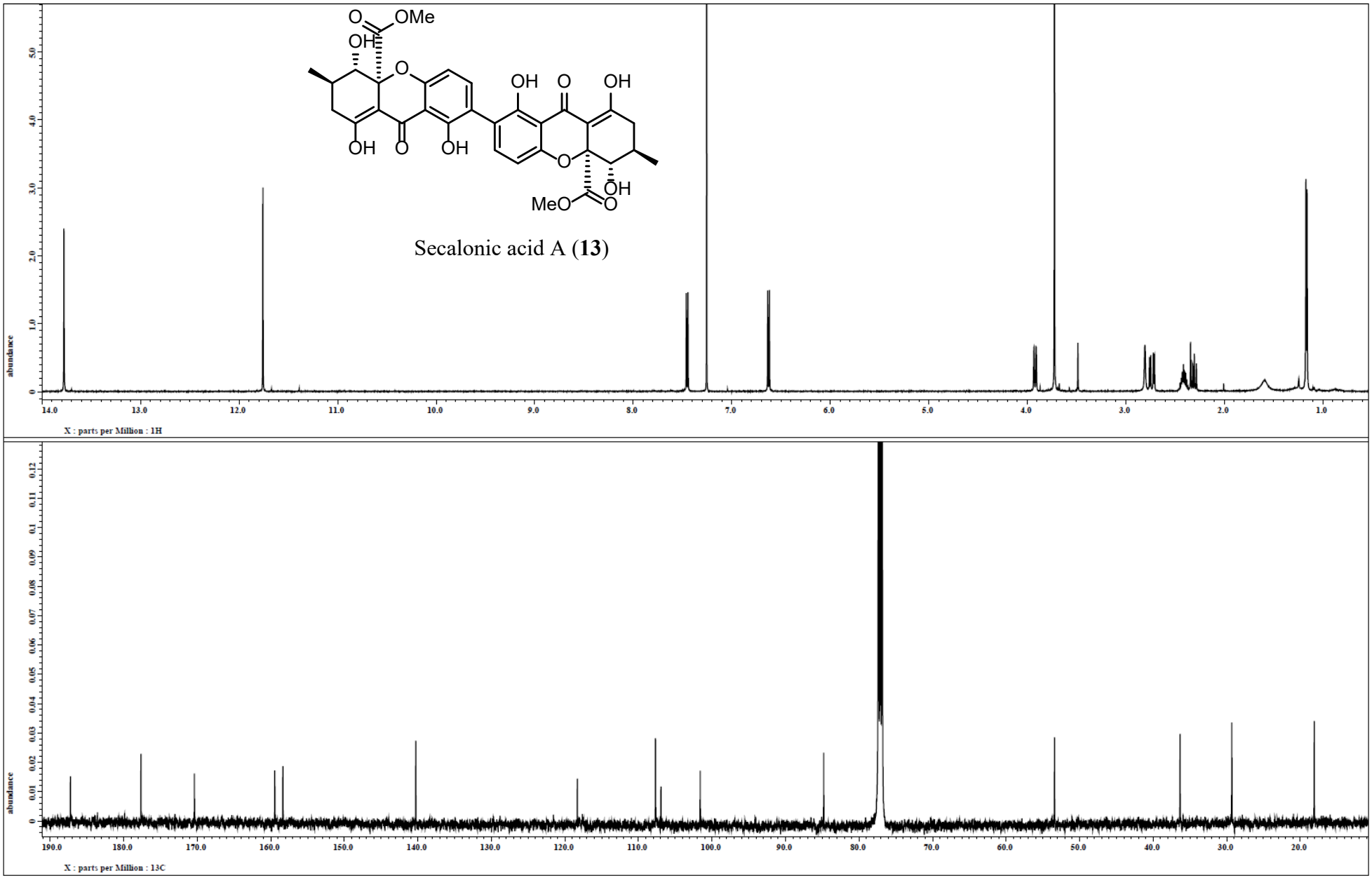

Figure S14. ^{1}H and ^{13}C NMR spectra of compound **13** [500 MHz for ^{1}H and 125 MHz for ^{13}C, $CDCl_3$].

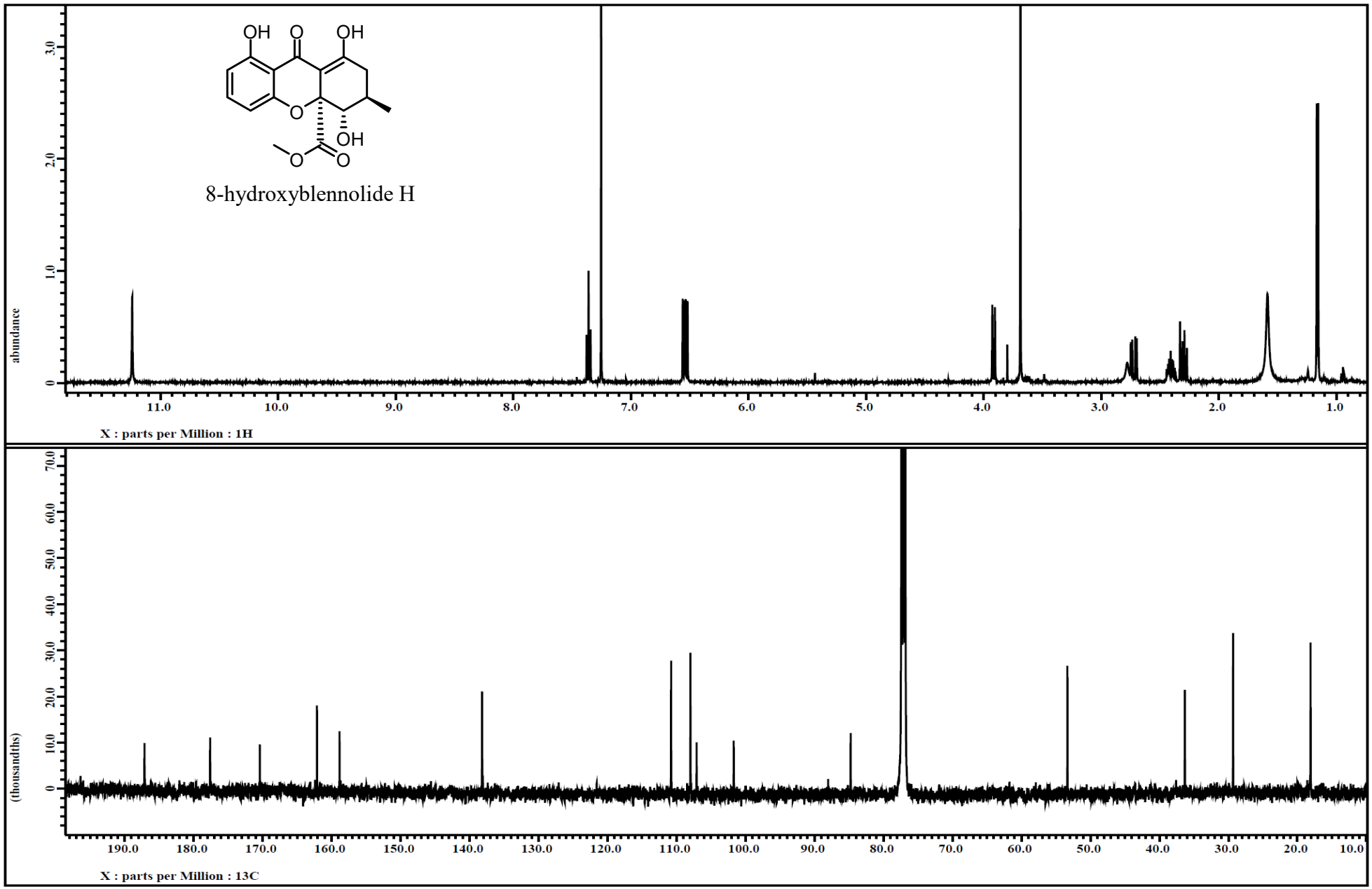

Figure S15. ^{1}H and ^{13}C NMR spectra of compound **14** [500 MHz for ^{1}H and 125 MHz for ^{13}C, $CDCl_3$].

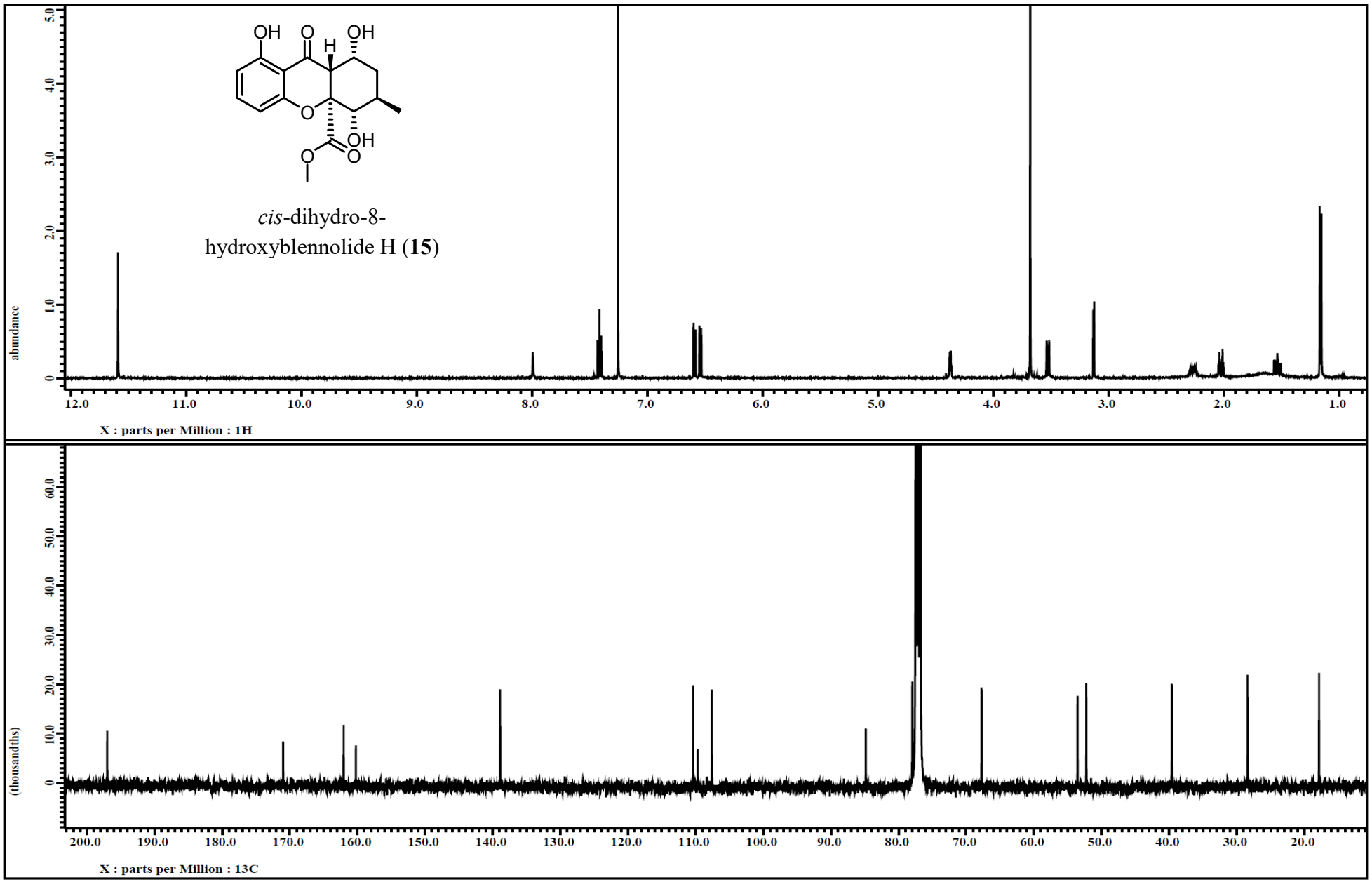

Figure S16. ^{1}H and ^{13}C NMR spectra of compound **15** [500 MHz for ^{1}H and 100 MHz for ^{13}C, $CDCl_3$].

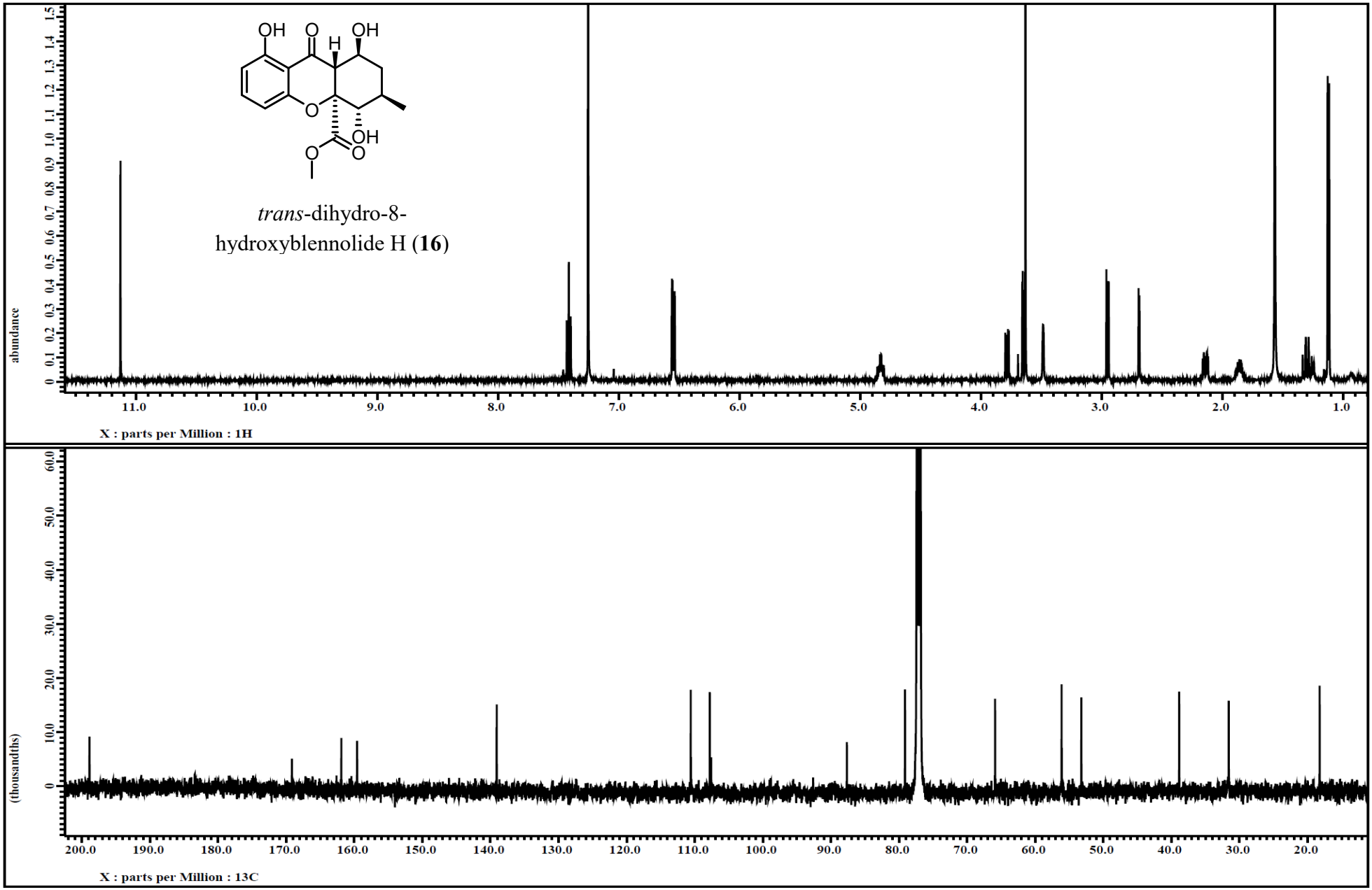

Figure S17. ^{1}H and ^{13}C NMR spectra of compound **16** [500 MHz for ^{1}H and 125 MHz for ^{13}C, $CDCl_3$].

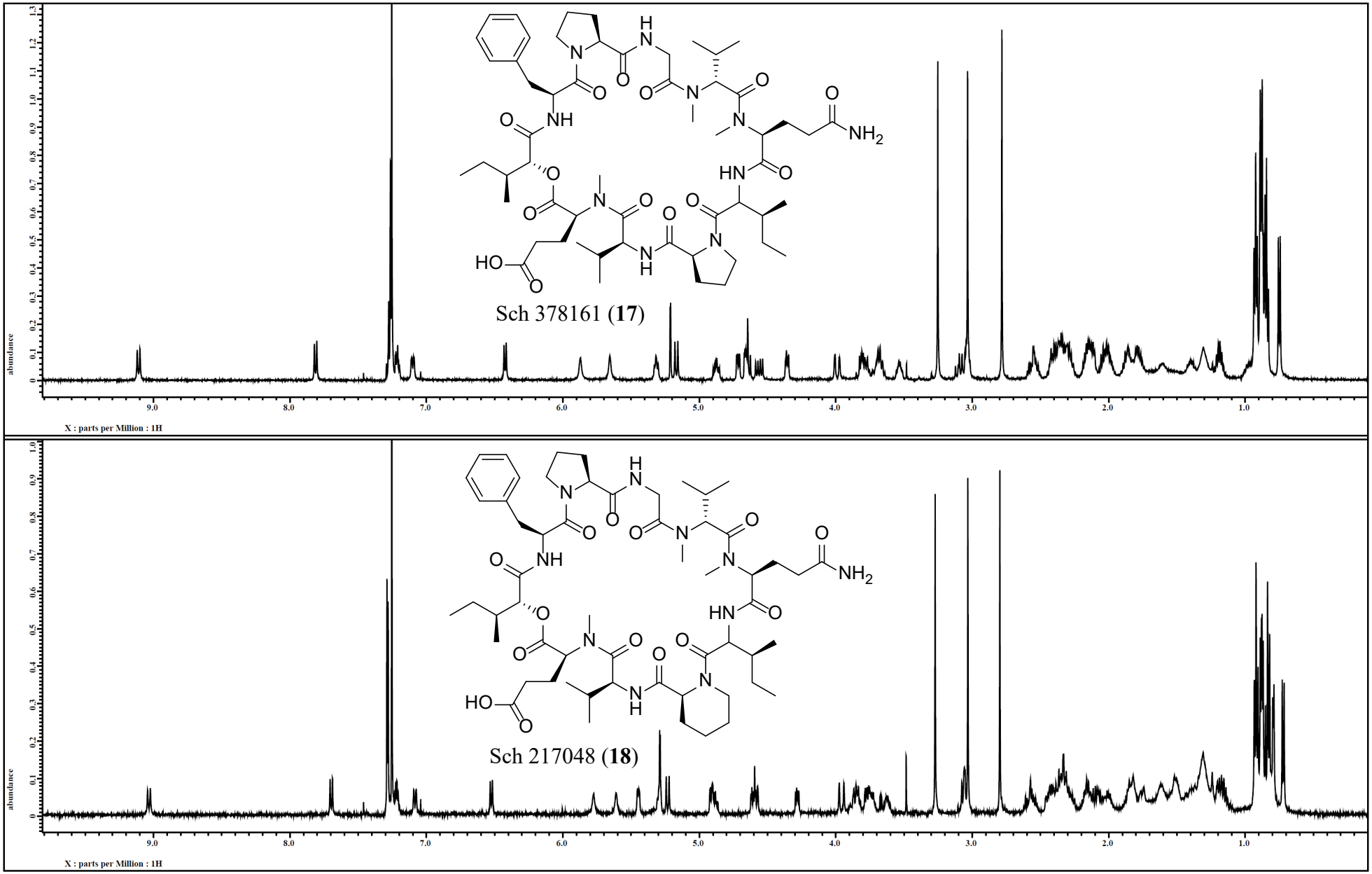

Figure S18. ^{1}H NMR spectra of compounds **17** and **18** [500 MHz, $CDCl_3$].

Table S3. Crystal data, data collection, and refinement details for compound 8

Crystal data	
$C_{10}H_{12}O_5$	$Z = 2$
$M_r = 212.20$	$F(000) = 224$
Triclinic, $P\bar{1}$	$D_x = 1.491$ Mg m^{-3}
$a = 4.1747$ (3) Å	Mo $K\alpha$ radiation, $\lambda = 0.71073$ Å
$b = 10.9965$ (7) Å	Cell parameters from 6326 reflections
$c = 11.0671$ (7) Å	$\theta = 3.8$–$30.0°$
$\alpha = 70.466$ (1)°	$\mu = 0.12$ mm^{-1}
$\beta = 85.814$ (1)°	$T = 193$ K
$\gamma = 80.816$ (1)°	Irregular, colourless
$V = 472.57$ (5) Å^3	0.28 × 0.24 × 0.13 mm
Data Collection	
Bruker APEX CCD diffractometer	5123 reflections with $I > 2\sigma(I)$
Radiation source: fine-focus sealed X-ray tube	$R_{int} = 0.019$
Graphite monochromator	$\theta_{max} = 30.1°$, $\theta_{min} = 3.8°$
ϕ and ω scans	$h = -5 \rightarrow 5$
8913 measured reflections	$k = -15 \rightarrow 15$
5255 independent reflections	$l = -15 \rightarrow 15$
Refinement	
Refinement on F^2	Hydrogen site location: mixed
Least-squares matrix: full	H atoms treated by a mixture of independent and constrained refinement
$R[F^2 > 2\sigma(F^2)] = 0.035$	$w = 1/[\sigma^2(F_o^2) + (0.0696P)^2 + 0.0318P]$ where $P = (F_o^2 + 2F_c^2)/3$
$wR(F^2) = 0.099$	$(\Delta/\sigma)_{max} < 0.001$
$S = 1.03$	$\Delta\rangle_{max} = 0.37$ e Å^{-3}
5255 reflections	$\Delta\rangle_{min} = -0.20$ e Å^{-3}
281 parameters	Absolute structure: It was not possible to unambiguously determine the absolute structure from X-ray data for this light atom structure. Results for Flack x using 2407 quotients [(I+)–(I–)]/[(I+)+(I–)] are given (Parsons and Flack (2004), Acta Cryst. A60, s61).
3 restraints	Absolute structure parameter: 0.1 (3)
Primary atom site location: structure-invariant direct methods	

Table S4. Antimicrobial activities of compounds 1, 4-18

Compound	Minimal Inhibitory Concentration (μg/mL)				
	S. aureus	***E. coli***	***M. smegmatis***	***C. albicans***	***A. niger***
1	> 203	> 203	> 203	> 203	203
4	> 140	> 140	> 140	> 140	> 140
5	> 25	> 25	> 25	> 25	> 25
6	> 145	> 145	145	145	> 145
7	> 155	> 155	> 155	> 155	> 155
8	> 53	> 53	> 53	> 53	> 53
9	> 55	> 55	> 55	> 55	> 55
10	> 35	> 35	> 35	> 35	> 35
11	> 25	25	25	25	> 25
12	> 75	75	> 75	> 75	> 75
13	> 75	> 75	> 75	> 75	> 75
14	> 65	> 65	> 65	> 65	> 65
15	> 100	> 100	> 100	100	>100
16	> 75	> 75	> 75	> 75	> 75
17	> 125	> 125	> 125	> 125	> 125
18	> 98	> 98	> 98	> 98	> 98

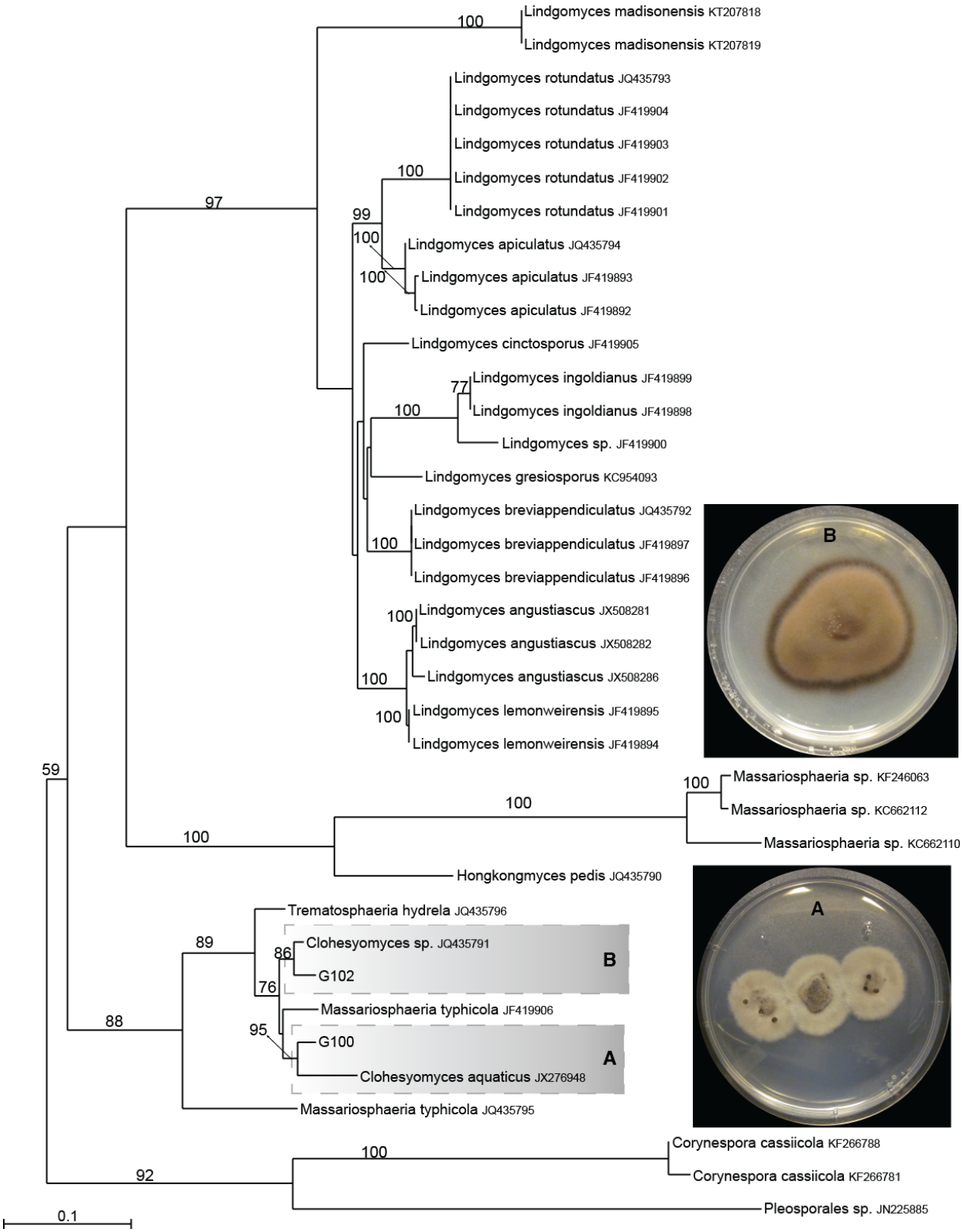

Figure S19. Phylogram of the most likely tree (-lnL = 7703.41) from a PHYML analysis of 37 taxa based on ITS rDNA (1087 bp). Numbers refer to RAxML bootstrap support values ≥ 70% based on 1000 replicates. G100 and G012 are highlighted in gray. 21 d old cultures of both isolates are shown (A, G100, *Clohesyomyces aquaticus*); (B, G012, *Clohesyomyces* sp.) Bar indicates nucleotide substitutions per site.

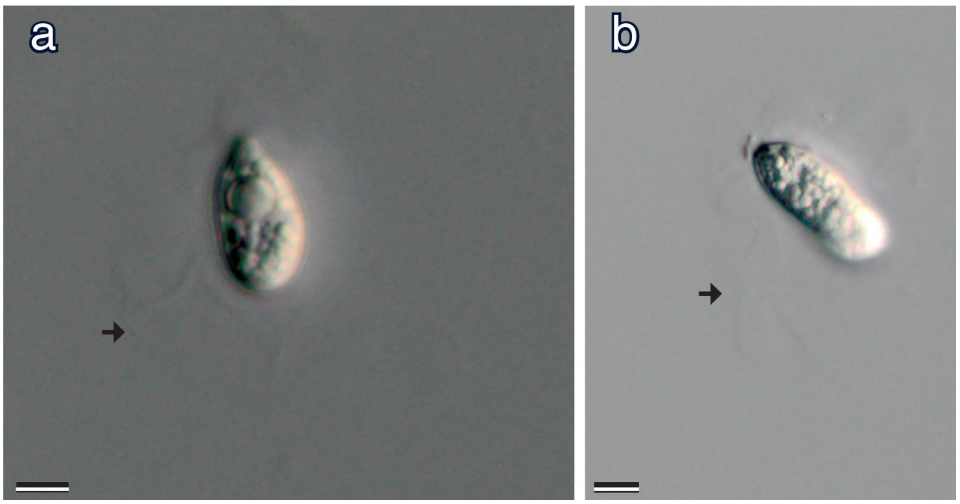

Figure S20. a–b. Conidia of *Clohesyomyces aquaticus* (G100); note arrow showing irregular mucilaginous sheath. Bars = 10 µm.